

Equivariant Symmetries for Inertial Navigation Systems

Alessandro Fornasier ^{a,*}, Yixiao Ge ^b, Pieter van Goor ^b, Robert Mahony ^b,
Stephan Weiss ^a

^aControl of Networked Systems Group, University of Klagenfurt, Austria

^bSystem Theory and Robotics Lab, Australian Centre for Robotic Vision, Australian National University, Australia

Abstract

This paper investigates the problem of inertial navigation system (INS) filter design through the lens of symmetry. The extended Kalman filter (EKF) and its variants, have been the staple of INS filtering for 50 years; however, recent advances in inertial navigation systems have exploited matrix Lie group structure to design stochastic filters and state observers that have been shown to display superior performance compared to classical solutions. In this work, we consider the case where a vehicle has an inertial measurement unit (IMU) and a global navigation satellite system (GNSS) receiver. We show that all the modern variants of the EKF for these sensors can be interpreted as the recently proposed Equivariant Filter (EqF) design methodology applied to different choices of symmetry group for the INS problem. This leads us to propose two new symmetries for the INS problem that have not been considered in the prior literature, and provide a discussion of the relative strengths and weaknesses of all the different algorithms. We believe the collection of symmetries that we present here capture all the sensible choices of symmetry for this problem and sensor suite, and that the analysis provided is indicative of the relative real-world performance potential of the different algorithms.

Key words: Inertial navigation system; Symmetry; Equivariance; Equivariant filter.

1 Introduction

The theory of invariant filtering for group affine systems [3, 2] and the theory of equivariant filters [15, 19, 24] that generalizes to systems on homogeneous spaces have provided general design frameworks, as well as strong theoretical performance guarantees, for filter designs that exploit symmetry. This has motivated the widespread use of invariant filters in the robotics community, and its adoption for inertial navigation problems [10, 22, 14]. The application of these principles to inertial navigation systems (INS) has seen the most significant performance gains from algorithm design in this field for the last 40 years. There are now several competing modern INS filters based on geometric insights available in the literature [1, 3, 9] and the question of how to analyse and evaluate the similarities and differences is now of interest. A recent paper by Barrau et al. states “*The big question when it comes to invariant*

observers/filters is how do we find a group structure for the state space [...]” [3]. The goal of the present paper is to convince the reader that the choice of symmetry structure is in fact the *only* difference between different versions of modern geometric INS filters.

In this paper we present six different symmetry groups that act on the state-space of the INS problem. We use the recent equivariant filter design methodology to generate INS filter algorithms for each of these symmetries. We show that the classical multiplicative extended Kalman filter (MEKF) [12], the Imperfect-invariant extended Kalman filter (IEKF) [1], the two-frame group invariant extended Kalman filter (TFG-IEKF) [3], and the authors own recent work proposing an equivariant filter for the tangent group structure (TG-EqF) [9] are all associated with equivariant filter design [25] applied to different symmetry actions on the same state-space. This leads us to consider the properties of the symmetry groups and suggests two additional symmetries leading to filters, that we term the Direct Position Equivariant Filter (DP-EqF) and Semi-Direct Bias Equivariant Filter (SD-EqF), that are novel and do not correspond to prior algorithms in the literature. We derive equivariant filter (EqF) algorithms for all of the different symmetries demonstrating that this approach provides a unify-

* Corresponding author

Email addresses: `alessandro.fornasier@aau.at` (Alessandro Fornasier), `yixiao.ge@anu.edu.au` (Yixiao Ge), `pieter.vangoor@anu.edu.au` (Pieter van Goor), `robert.mahony@anu.edu.au` (Robert Mahony), `stephan.weiss@aau.at` (Stephan Weiss).

ing analysis framework for modern INS filters. In doing this we also make a minor contribution in demonstrating how fixed-frame measurements can be reformulated as body-frame relative measurements. This allows us to exploit output equivariance [25] for all the filter geometries ensuring at least third-order linearization error in the output equations.

We undertake a simple comparative study in concert with a linearization analysis of the error equations. Care should be taken in making general statements based on initial analysis; however, the key conclusions that we make are:

- The classical MEKF demonstrates noticeable performance limitations compared to the modern filters. In particular, it demonstrates worse transient response and reports significant overconfidence during the transient phase.
- The performance differences in modern filters are primarily visible during the transient phase of error response. The asymptotic behaviour of all filters is similar.
- Notwithstanding the above, the asymptotic performance of the TG-EqF appears superior to all other filters demonstrating the best consistency and the lowest error.
- The TG-EqF filter is the only filter with exact linearization of the navigation states, with the nonlinearities shifted to the bias states. The authors believe that this property underlies its asymptotic performance advantage.
- The bias state transient response of the filters with semi-direct bias symmetry (TG-EqF, DP-EqF and SD-EqF) appears superior to that of filters without this geometric structure (MEKF, IEKF and TFG-IEKF).

The study concludes that any of the IEKF, TG-EqF, DP-EqF, and SD-EqF filters are candidates for a high-performance INS filter design. The lower filter error and energy properties of the TG-EqF recommend it as the primary choice, although the authors note that this filter also involves an over-parameterization of the state that is not present in the other filters.

2 Notation and Mathematical Preliminaries

In this paper bold lowercase letters are used to indicate vector quantities. Bold capital letters are used to indicate matrices. Regular letters are used to indicate elements of a symmetry group.

Frames of reference are denoted as $\{A\}$ and $\{B\}$. Vectors describing physical quantities expressed in a frame of reference $\{A\}$ are denoted by ${}^A\mathbf{x}$. Rotation matrices encoding the orientation of a frame of reference $\{B\}$ with

respect to a reference $\{A\}$ are denoted by ${}^A\mathbf{R}_B$; in particular, ${}^A\mathbf{R}_B$ expresses a vector ${}^B\mathbf{x}$ defined in the $\{B\}$ frame of reference into a vector ${}^A\mathbf{x} = {}^A\mathbf{R}_B {}^B\mathbf{x}$ expressed in the $\{A\}$ frame of reference. Finally, $\mathbf{I}_n \in \mathbb{R}^{n \times n}$ is the $n \times n$ identity matrix, and $\mathbf{0}_{n \times m} \in \mathbb{R}^{n \times m}$ is the $n \times m$ zero matrix.

2.1 Lie theory

A Lie group \mathbf{G} is a smooth manifold endowed with a smooth group structure. For any $X, Y \in \mathbf{G}$, the group multiplication is denoted XY , the group inverse X^{-1} and the identity element I .

Given a Lie group \mathbf{G} , \mathcal{G} denotes the \mathbf{G} -Torsor [16], which is defined as the set of elements of \mathbf{G} (the underlying manifold), but without the group structure.

For a given Lie group \mathbf{G} , the Lie algebra \mathfrak{g} can be modelled as a vector space corresponding to the tangent space at the identity of the group, together with a bilinear non-associative map $[\cdot, \cdot] : \mathfrak{g} \rightarrow \mathfrak{g}$ called the *Lie bracket*. For a matrix Lie group, the Lie bracket is equal to the matrix commutator:

$$[\eta, \kappa] = \eta\kappa - \kappa\eta,$$

for any $\eta, \kappa \in \mathfrak{g} \subset \mathbb{R}^{n \times n}$.

The Lie algebra \mathfrak{g} is isomorphic to a vector space \mathbb{R}^n of dimension $n = \dim(\mathfrak{g})$. Define the *wedge* map and its inverse, the *vee* map, as linear mappings between the vector space and the Lie algebra:

$$(\cdot)^\wedge : \mathbb{R}^n \rightarrow \mathfrak{g}, \quad (\cdot)^\vee : \mathfrak{g} \rightarrow \mathbb{R}^n.$$

For any $X, Y \in \mathbf{G}$, define the left and right translation

$$\begin{aligned} L_X : \mathbf{G} &\rightarrow \mathbf{G}, & L_X(Y) &= XY, \\ R_X : \mathbf{G} &\rightarrow \mathbf{G}, & R_X(Y) &= YX. \end{aligned}$$

In this paper, we will limit our consideration to matrix Lie-groups and products of matrix Lie-groups, although the results are expected to hold on a larger class of groups.

The Adjoint map for the group \mathbf{G} , $\text{Ad}_X : \mathfrak{g} \rightarrow \mathfrak{g}$ is defined by

$$\text{Ad}_X[\mathbf{u}^\wedge] = dL_X dR_{X^{-1}}[\mathbf{u}^\wedge],$$

for every $X \in \mathbf{G}$ and $\mathbf{u}^\wedge \in \mathfrak{g}$, where dL_X , and dR_X denote the differentials of the left, and right translation,

respectively. Given particular wedge and vee maps, the Adjoint matrix is defined as the map $\mathbf{Ad}_X^\vee : \mathbb{R}^n \rightarrow \mathbb{R}^n$

$$\mathbf{Ad}_X^\vee \mathbf{u} = (\text{Ad}_X [\mathbf{u}^\wedge])^\vee.$$

Note that for general groups constructed of products of matrix Lie groups, the Adjoint map cannot be directly expressed in the form $X\mathbf{u}^\wedge X^{-1}$.

In addition to the Adjoint map for the group \mathbf{G} , the adjoint map for the Lie algebra \mathfrak{g} can be defined as the differential at the identity of the Adjoint map for the group \mathbf{G} . The adjoint map for the Lie algebra $\text{ad}_{\mathbf{u}^\wedge} : \mathfrak{g} \rightarrow \mathfrak{g}$ is given by

$$\text{ad}_{\mathbf{u}^\wedge} [\mathbf{v}^\wedge] = [\mathbf{u}^\wedge, \mathbf{v}^\wedge],$$

and is equivalent to the Lie bracket. Given particular wedge and vee maps, we define the adjoint matrix $\mathbf{ad}_{\mathbf{u}^\wedge}^\vee : \mathbb{R}^n \rightarrow \mathbb{R}^n$ to be

$$\mathbf{ad}_{\mathbf{u}^\wedge}^\vee \mathbf{v} = (\mathbf{u}^\wedge \mathbf{v}^\wedge - \mathbf{v}^\wedge \mathbf{u}^\wedge)^\vee = [\mathbf{u}^\wedge, \mathbf{v}^\wedge]^\vee.$$

Note that for a group constructed of products of matrix Lie groups, the adjoint map is not the matrix commutator. For all $\mathbf{u}, \mathbf{v} \in \mathbb{R}^n$ and $X \in \mathbf{G}$, the two adjoints commute:

$$\begin{aligned} \text{Ad}_X [\text{ad}_{\mathbf{u}^\wedge} [\mathbf{v}^\wedge]] &= \text{ad}_{(\text{Ad}_X [\mathbf{u}^\wedge])} [\text{Ad}_X [\mathbf{v}^\wedge]], \\ \mathbf{Ad}_X^\vee \mathbf{ad}_{\mathbf{u}^\wedge}^\vee \mathbf{v} &= \mathbf{ad}_{\text{Ad}_X^\vee \mathbf{u}^\wedge}^\vee \mathbf{Ad}_X^\vee \mathbf{v}, \end{aligned}$$

A semi-direct product group $\mathbf{G} \ltimes \mathbf{H}$ can be seen as a generalization of the direct product group $\mathbf{G} \times \mathbf{H}$ where the underlying set is given by the cartesian product of two groups \mathbf{G} and \mathbf{H} . Contrary to the direct product, in the semi-direct product, the group multiplication is defined with the group \mathbf{G} that acts on a group \mathbf{H} by a group automorphism.

In this work we will consider a semi-direct product symmetry group [21], [19], [20] $\mathbf{G}_\mathfrak{g}^\times := \mathbf{G} \ltimes \mathfrak{g}$ where \mathfrak{g} is the Lie algebra of \mathbf{G} , or a subalgebra of \mathbf{G} , that is, a vector space group under addition. Let $A, B \in \mathbf{G}$ and $a, b \in \mathfrak{g}$ and define $X = (A, a)$ and $Y = (B, b)$ elements of the symmetry group $\mathbf{G}_\mathfrak{g}^\times$. Group multiplication is defined to be the semi-direct product $YX = (BA, b + \text{Ad}_B [a])$. The inverse element is $X^{-1} = (A^{-1}, -\text{Ad}_{A^{-1}} [a])$ and identity element is $(I, 0)$.

2.2 Lie group action and homogeneous space

A right group action of a Lie group \mathbf{G} on a differentiable manifold \mathcal{M} is a smooth map $\phi : \mathbf{G} \times \mathcal{M} \rightarrow \mathcal{M}$ that satisfies

$$\phi(I, \xi) = \xi, \quad \phi(X, \phi(Y, \xi)) = \phi(YX, \xi),$$

for any $X, Y \in \mathbf{G}$ and $\xi \in \mathcal{M}$. A right group action ϕ induces a family of diffeomorphism $\phi_X : \mathcal{M} \rightarrow \mathcal{M}$ and smooth projections $\phi_\xi : \mathbf{G} \rightarrow \mathcal{M}$. The group action ϕ is said to be transitive if the induced projection ϕ_ξ is surjective. In this case, \mathcal{M} is a homogeneous space of \mathbf{G} .

2.3 Useful maps

For all $\mathbf{x} \in \mathbb{R}^n$ define the maps:

$$\begin{aligned} \overline{(\cdot)} : \mathbb{R}^n &\rightarrow \mathbb{R}^{n+3}, & \mathbf{x} &\mapsto \overline{\mathbf{x}} = (\mathbf{0}_{3 \times 1}, \mathbf{x}), \\ \underline{(\cdot)} : \mathbb{R}^n &\rightarrow \mathbb{R}^{n+3}, & \mathbf{x} &\mapsto \underline{\mathbf{x}} = (\mathbf{x}, \mathbf{0}_{3 \times 1}). \end{aligned}$$

For all $X = (A, a, b) \in \mathbf{SE}_2(3) \mid A \in \mathbf{SO}(3), a, b \in \mathbb{R}^3$, define the map:

$$\Omega(\cdot) : \mathbf{SE}_2(3) \rightarrow \mathfrak{se}_2(3), \quad \Omega(X) = (\mathbf{0}_{3 \times 1}, \mathbf{0}_{3 \times 1}, a)^\wedge \in \mathfrak{se}_2(3).$$

For all $\mathbf{a}, \mathbf{b}, \mathbf{c} \in \mathbb{R}^3 \mid (\mathbf{a}, \mathbf{b}, \mathbf{c}) \in \mathbb{R}^9$, define the map:

$$\Pi(\cdot) : \mathfrak{se}_2(3) \rightarrow \mathfrak{se}(3), \quad \Pi((\mathbf{a}, \mathbf{b}, \mathbf{c})^\wedge) = (\mathbf{a}, \mathbf{b})^\wedge \in \mathfrak{se}(3).$$

3 The Biased Inertial Navigation Problem

Consider a mobile robot equipped with an IMU providing angular velocity and acceleration measurements, as well as other sensors providing partial direct or indirect state measurements (e.g. a GNSS receiver providing position measurements or a magnetometer providing direction measurements). Let $\{G\}$ denote the global inertial frame of reference and $\{I\}$ denote the IMU frame of reference. In non-rotating, flat earth assumption, the deterministic (noise-free) continuous-time biased inertial navigation system is

$${}^G \dot{\mathbf{R}}_I = {}^G \mathbf{R}_I ({}^I \boldsymbol{\omega} - {}^I \mathbf{b}_\omega)^\wedge, \quad (1a)$$

$${}^G \dot{\mathbf{v}}_I = {}^G \mathbf{R}_I ({}^I \mathbf{a} - {}^I \mathbf{b}_a) + {}^G \mathbf{g}, \quad (1b)$$

$${}^G \dot{\mathbf{p}}_I = {}^G \mathbf{v}_I, \quad (1c)$$

$${}^I \dot{\mathbf{b}}_\omega = {}^I \boldsymbol{\tau}_\omega, \quad (1d)$$

$${}^I \dot{\mathbf{b}}_a = {}^I \boldsymbol{\tau}_a. \quad (1e)$$

Here, ${}^G \mathbf{R}_I$ denotes the rigid body orientation, and ${}^G \mathbf{p}_I$ and ${}^G \mathbf{v}_I$ denote the rigid body position and velocity expressed in the $\{G\}$ frame, respectively. These variables are termed the *navigation states*. The gravity vector ${}^G \mathbf{g}$ is expressed in frame $\{G\}$. The gyroscope measurement and accelerometer measurement are written ${}^I \boldsymbol{\omega}$ and ${}^I \mathbf{a}$ respectively. The two biases ${}^I \mathbf{b}_\omega$ and ${}^I \mathbf{b}_a$ are termed the *bias states*. The inputs $\boldsymbol{\tau}_\omega, \boldsymbol{\tau}_a$ are used to model the biases' dynamics, and are zero when the biases are modeled as constant quantities.

Table 1
Descriptive-Lean Notation Conversion Table.

Description	Descriptive notation	Lean notation
Rigid body orientation	${}^G\mathbf{R}_I$	\mathbf{R}
Rigid body velocity	${}^G\mathbf{v}_I$	\mathbf{v}
Rigid body position	${}^G\mathbf{p}_I$	\mathbf{p}
Angular velocity measurement	${}^I\boldsymbol{\omega}$	$\boldsymbol{\omega}$
Gyroscope bias	${}^I\mathbf{b}_\omega$	\mathbf{b}_ω
Acceleration measurement	${}^I\mathbf{a}$	\mathbf{a}
Accelerometer bias	${}^I\mathbf{b}_a$	\mathbf{b}_a

The state space is $\mathcal{M} = \mathcal{SO}(3) \times \mathbb{R}^3 \times \mathbb{R}^3 \times \mathbb{R}^3 \times \mathbb{R}^3$ where the 4 copies of \mathbb{R}^3 model velocity, position, and angular and acceleration bias, respectively, and $\mathcal{SO}(3)$ is the $\mathbf{SO}(3)$ -torsor with rotation matrices representing coordinates of orientation rather than physical rotation of space. Note that the state space itself is not a Lie-group in the EqF formulation. Rather symmetry is modeled as a group action on \mathcal{M} , allowing us to consider different symmetries acting on the same INS state. We write an element of the state space, and an element of the input space respectively

$$\xi = ({}^G\mathbf{R}_I, {}^G\mathbf{v}_I, {}^G\mathbf{p}_I, {}^I\mathbf{b}_\omega, {}^I\mathbf{b}_a) \in \mathcal{M}, \quad (2)$$

$$u = ({}^I\boldsymbol{\omega}, {}^I\mathbf{a}, {}^I\boldsymbol{\tau}_\omega, {}^I\boldsymbol{\tau}_a) \in \mathbb{L} \subset \mathbb{R}^{12}. \quad (3)$$

For the sake of clarity of the presentation, in the following sections, we drop subscripts and superscripts from state, input and output variables, and adopt the lean notation defined in Table 1.

4 INS Symmetries

In the following subsections, we analyze different symmetries of the biased inertial navigation system under the lens of equivariance; that is, we show how those symmetries relate to classical filter design when exploited within the equivariant filter framework, and how every filter is an EqF under an appropriate choice of symmetry. Starting with Tab. 2, we show the relation between INS filters and symmetry group, as well as the differences in the state error linearization of filters built upon those symmetries. In Sec. 4.1, 4.2 and 4.3, we discuss the symmetry groups that lead to the design of equivariant filters equivalent to the widely-known MEKF, IEKF, and the recently published TFG-IEKF. In Sec. 4.4 we briefly recall the tangent group recently introduced and exploited for INS in our prior work [9, 8]. In Sec. 4.5 and 4.6, we introduce two new symmetry groups for biased inertial navigation Systems. These groups are based on the semi-direct product and aim to address the over-parametrization of bias states introduced in our prior work [9].

4.1 Special Orthogonal group $\mathbf{G}_O : \mathbf{SO}(3) \times \mathbb{R}^{12}$

Lie group theory was first applied to navigation systems to overcome the limitation and the singularities of using Euler angles as the parameterization of the attitude of a rigid body. Originally formulated on the quaternion group, the modern approach directly models attitude on the Special Orthogonal group $\mathbf{SO}(3)$.

Define the symmetry group $\mathbf{G}_O := \mathbf{SO}(3) \times \mathbb{R}^{12}$, and let $X = (A, a, b, \alpha, \beta) \in \mathbf{G}_O$, where $A \in \mathbf{SO}(3)$, $a, b, \alpha, \beta \in \mathbb{R}^3$. Let $X = (A_X, a_X, b_X, \alpha_X, \beta_X)$, $Y = (A_Y, a_Y, b_Y, \alpha_Y, \beta_Y)$ be two elements of the symmetry group, then the group product is written $XY = (A_X A_Y, a_X + a_Y, b_X + b_Y, \alpha_X + \alpha_Y, \beta_X + \beta_Y)$. The inverse of an element X is given by $X^{-1} = (A^T, -a, -b, -\alpha, -\beta)$.

Lemma 1 Define $\phi : \mathbf{G}_O \times \mathcal{M} \rightarrow \mathcal{M}$ as

$$\phi(X, \xi) := (\mathbf{R}A, \mathbf{v} + a, \mathbf{p} + b, \boldsymbol{\omega} + \alpha, \mathbf{b}_a + \beta) \in \mathcal{M}. \quad (4)$$

Then, ϕ is a transitive right group action of \mathbf{G}_O on \mathcal{M} .

The existence of a transitive group action of the symmetry group \mathbf{G}_O on the state space \mathcal{M} guarantees the existence of a lift [15].

Theorem 2 Define the map $\Lambda : \mathcal{M} \times \mathbb{L} \rightarrow \mathfrak{g}_O$ by

$$\Lambda(\xi, u) := (\Lambda_1(\xi, u), \dots, \Lambda_5(\xi, u)).$$

where $\Lambda_1 : \mathcal{M} \times \mathbb{L} \rightarrow \mathfrak{so}(3)$, and $\Lambda_2, \dots, \Lambda_5 : \mathcal{M} \times \mathbb{L} \rightarrow \mathbb{R}^3$ are given by

$$\Lambda_1(\xi, u) := ({}^I\boldsymbol{\omega} - {}^I\mathbf{b}_\omega)^\wedge, \quad (5)$$

$$\Lambda_2(\xi, u) := {}^G\mathbf{R}_I ({}^I\mathbf{a} - {}^I\mathbf{b}_a) + {}^G\mathbf{g}, \quad (6)$$

$$\Lambda_3(\xi, u) := {}^G\mathbf{v}_I, \quad (7)$$

$$\Lambda_4(\xi, u) := {}^I\boldsymbol{\tau}_\omega, \quad (8)$$

$$\Lambda_5(\xi, u) := {}^I\boldsymbol{\tau}_a. \quad (9)$$

Then, the Λ is a lift for the system in Equ. (1) with respect to the symmetry group $\mathbf{G}_O := \mathbf{SO}(3) \times \mathbb{R}^{12}$.

In the appendix, it is shown that an EqF designed using this symmetry results in the well-known MEKF [12].

4.2 Extended Special Euclidean group $\mathbf{G}_{ES} : \mathbf{SE}_2(3) \times \mathbb{R}^6$

Using the extended pose $\mathbf{SE}_2(3)$ group to model the navigation states of the INS problem is one of the major developments in INS filtering in the last 10 years.

Define $\xi = (\mathbf{T}, \mathbf{b}) \in \mathcal{M} := \mathcal{SE}_2(3) \times \mathbb{R}^6$ to be the state space of the system. $\mathbf{T} = (\mathbf{R}, \mathbf{v}, \mathbf{p}) \in \mathcal{SE}_2(3)$ is the

Table 2

Qualitative overview of the differences in the presented symmetries when exploited for filter design.

Filter	Symmetry group	State error linearization.	$\mathbf{A} \mid \dot{\boldsymbol{\varepsilon}} \simeq \mathbf{A} \boldsymbol{\varepsilon}$
MEKF [12]	Special Orthogonal group $\mathbf{G}_O : \mathbf{SO}(3) \times \mathbb{R}^{12}$	State-dependent attitude error dynamics. State-dependent and input-dependent velocity error dynamics. Linear time-invariant position error dynamics. Linear time-invariant bias error dynamics	$\dot{\boldsymbol{\varepsilon}}_R \simeq -\hat{\mathbf{R}} \boldsymbol{\varepsilon}_{b_\omega} + \mathcal{O}(\boldsymbol{\varepsilon}^2),$ $\dot{\boldsymbol{\varepsilon}}_v \simeq -(\hat{\mathbf{R}}(\mathbf{a} - \hat{\mathbf{b}}_a))^\wedge \boldsymbol{\varepsilon}_R - \hat{\mathbf{R}} \boldsymbol{\varepsilon}_{b_a} + \mathcal{O}(\boldsymbol{\varepsilon}^2),$ $\dot{\boldsymbol{\varepsilon}}_p \simeq \boldsymbol{\varepsilon}_v,$ $\dot{\boldsymbol{\varepsilon}}_b = \mathbf{0}.$
Imperfect-IEKF [1]	Extended Special Euclidean group $\mathbf{G}_{ES} : \mathbf{SE}_2(3) \times \mathbb{R}^6$	State-dependent attitude, position and velocity error dynamics. Linear time-invariant bias error dynamics	$\dot{\boldsymbol{\varepsilon}}_R \simeq -\hat{\mathbf{R}} \boldsymbol{\varepsilon}_{b_\omega} + \mathcal{O}(\boldsymbol{\varepsilon}^2),$ $\dot{\boldsymbol{\varepsilon}}_v \simeq \mathbf{g}^\wedge \boldsymbol{\varepsilon}_R - \hat{\mathbf{v}}^\wedge \hat{\mathbf{R}} \boldsymbol{\varepsilon}_{b_\omega} - \hat{\mathbf{R}} \boldsymbol{\varepsilon}_{b_a} + \mathcal{O}(\boldsymbol{\varepsilon}^2),$ $\dot{\boldsymbol{\varepsilon}}_p \simeq \boldsymbol{\varepsilon}_v - \hat{\mathbf{p}}^\wedge \hat{\mathbf{R}} \boldsymbol{\varepsilon}_{b_\omega} + \mathcal{O}(\boldsymbol{\varepsilon}^2),$ $\dot{\boldsymbol{\varepsilon}}_b = \mathbf{0}.$
TFG-IEKF [3]	Two-Frame group $\mathbf{G}_{TF} : \mathbf{SO}(3) \times (\mathbb{R}^6 \oplus \mathbb{R}^6)$	Linear time-invariant attitude error dynamics. State-dependent velocity and position error dynamics. State-dependent and input-dependent bias error dynamics	$\dot{\boldsymbol{\varepsilon}}_R \simeq \boldsymbol{\varepsilon}_{b_\omega},$ $\dot{\boldsymbol{\varepsilon}}_v \simeq \mathbf{g}^\wedge \boldsymbol{\varepsilon}_R + \hat{\mathbf{v}}^\wedge \boldsymbol{\varepsilon}_{b_\omega} + \boldsymbol{\varepsilon}_{b_a} + \mathcal{O}(\boldsymbol{\varepsilon}^2),$ $\dot{\boldsymbol{\varepsilon}}_p \simeq \boldsymbol{\varepsilon}_v + \hat{\mathbf{p}}^\wedge \boldsymbol{\varepsilon}_{b_\omega} + \mathcal{O}(\boldsymbol{\varepsilon}^2),$ $\dot{\boldsymbol{\varepsilon}}_{b_\omega} \simeq (\hat{\mathbf{R}}(\boldsymbol{\omega} - \hat{\mathbf{b}}_\omega))^\wedge \boldsymbol{\varepsilon}_{b_\omega} + \mathcal{O}(\boldsymbol{\varepsilon}^2),$ $\dot{\boldsymbol{\varepsilon}}_{b_a} \simeq (\hat{\mathbf{R}}(\boldsymbol{\omega} - \hat{\mathbf{b}}_\omega))^\wedge \boldsymbol{\varepsilon}_{b_a} + \mathcal{O}(\boldsymbol{\varepsilon}^2).$
TG-EqF [9]	Tangent group $\mathbf{G}_{TG} : \mathbf{SE}_2(3) \times \mathfrak{se}_2(3)$	Linear time-invariant attitude, velocity and position error dynamics. State-dependent and input-dependent bias error dynamics	$\dot{\boldsymbol{\varepsilon}}_R \simeq \boldsymbol{\varepsilon}_{b_\omega},$ $\dot{\boldsymbol{\varepsilon}}_v \simeq \mathbf{g}^\wedge \boldsymbol{\varepsilon}_R + \boldsymbol{\varepsilon}_{b_a},$ $\dot{\boldsymbol{\varepsilon}}_p \simeq \boldsymbol{\varepsilon}_v + \boldsymbol{\varepsilon}_{b_\nu},$ $\dot{\boldsymbol{\varepsilon}}_b \simeq \mathbf{ad}_{(\hat{\mathbf{w}}^\wedge + \mathbf{G})}^\vee \boldsymbol{\varepsilon}_b + \mathcal{O}(\boldsymbol{\varepsilon}^2).$
DP-EqF	Direct Position group ² $\mathbf{G}_{DP} : \mathbf{HG}(3) \times \mathfrak{hg}(3) \times \mathbb{R}^3$	Linear time-invariant attitude and velocity error dynamics. State-dependent and input-dependent position and bias error dynamics	$\dot{\boldsymbol{\varepsilon}}_R \simeq \boldsymbol{\varepsilon}_{b_\omega},$ $\dot{\boldsymbol{\varepsilon}}_v \simeq \mathbf{g}^\wedge \boldsymbol{\varepsilon}_R + \boldsymbol{\varepsilon}_{b_a},$ $\dot{\boldsymbol{\varepsilon}}_p \simeq \boldsymbol{\varepsilon}_v + \hat{\mathbf{v}}^\wedge \boldsymbol{\varepsilon}_R + \mathcal{O}(\boldsymbol{\varepsilon}^2),$ $\dot{\boldsymbol{\varepsilon}}_b \simeq \mathbf{ad}_{(\hat{\mathbf{w}}^\wedge + \mathbf{G})}^\vee \boldsymbol{\varepsilon}_b + \mathcal{O}(\boldsymbol{\varepsilon}^2).$
SD-EqF	Semi-Direct Bias group $\mathbf{G}_{SD} : \mathbf{SE}_2(3) \times \mathfrak{se}(3)$	Linear time-invariant attitude and velocity error dynamics. State-dependent position error dynamics. State-dependent and input-dependent bias error dynamics	$\dot{\boldsymbol{\varepsilon}}_R \simeq \boldsymbol{\varepsilon}_{b_\omega},$ $\dot{\boldsymbol{\varepsilon}}_v \simeq \mathbf{g}^\wedge \boldsymbol{\varepsilon}_R + \boldsymbol{\varepsilon}_{b_a},$ $\dot{\boldsymbol{\varepsilon}}_p \simeq \boldsymbol{\varepsilon}_v + \hat{\mathbf{p}}^\wedge \boldsymbol{\varepsilon}_{b_\omega} + \mathcal{O}(\boldsymbol{\varepsilon}^2),$ $\dot{\boldsymbol{\varepsilon}}_b \simeq \mathbf{ad}_{(\hat{\mathbf{w}}^\wedge + \mathbf{G})}^\vee \boldsymbol{\varepsilon}_b + \mathcal{O}(\boldsymbol{\varepsilon}^2).$

extended pose [5], which includes the orientation the, velocity and the position of the rigid body, whereas $\mathbf{b} = (\mathbf{b}_\omega, \mathbf{b}_a) \in \mathbb{R}^6$ denotes the IMU biases. Let $u = (\mathbf{w}, \boldsymbol{\tau}) \in \mathbb{L} \subseteq \mathbb{R}^{12}$ denote the system input, where $\mathbf{w} = (\boldsymbol{\omega}, \mathbf{a}) \in \mathbb{R}^6$ denotes the input given by the IMU readings, and $\boldsymbol{\tau} = (\boldsymbol{\tau}_\omega, \boldsymbol{\tau}_a) \in \mathbb{R}^6$ denotes the input for the IMU biases. Define the matrices

$$\begin{aligned} \mathbf{G} &= (\underline{\mathbf{g}})^\wedge \in \mathfrak{se}_2(3), \\ \mathbf{B} &= (\underline{\mathbf{b}})^\wedge \in \mathfrak{se}_2(3), \\ \mathbf{W} &= (\underline{\mathbf{w}})^\wedge \in \mathfrak{se}_2(3), \end{aligned} \quad \mathbf{D} = \begin{bmatrix} \mathbf{0}_{3 \times 3} & \mathbf{0}_{3 \times 1} & \mathbf{0}_{3 \times 1} \\ \mathbf{0}_{1 \times 3} & 0 & 1 \\ \mathbf{0}_{1 \times 3} & 0 & 0 \end{bmatrix} \in \mathbb{R}^{5 \times 5}.$$

² The homogeneous Galilean group $\mathbf{HG}(3)$ is isomorphic to $\mathbf{SE}(3)$ but acts on attitude and velocity rather than attitude and position.

Then, the system in Equ. (1) may then be written as

$$\dot{\mathbf{T}} = \mathbf{T}(\mathbf{W} - \mathbf{B} + \mathbf{D}) + (\mathbf{G} - \mathbf{D})\mathbf{T}, \quad (10a)$$

$$\dot{\mathbf{b}} = \boldsymbol{\tau}. \quad (10b)$$

Define the symmetry group $\mathbf{G}_{ES} := \mathbf{SE}_2(3) \times \mathbb{R}^6$, and let $X = (C, \gamma) \in \mathbf{G}_{ES}$, where $C = (A, a, b) \in \mathbf{SE}_2(3)$, $A \in \mathbf{SO}(3)$, $a, b \in \mathbb{R}^3$, $\gamma \in \mathbb{R}^6$. Let $X = (C_X, \gamma_X)$, $Y = (C_Y, \gamma_Y)$ be two elements of the symmetry group, then the group product is written $XY = (C_X C_Y, \gamma_X + \gamma_Y)$. The inverse of an element X is given by $X^{-1} = (C^{-1}, -\gamma)$.

Lemma 3 Define $\phi : \mathbf{G}_{ES} \times \mathcal{M} \rightarrow \mathcal{M}$ as

$$\phi(X, \xi) := (\mathbf{T}C, \mathbf{b} + \gamma) \in \mathcal{M}. \quad (11)$$

Then, ϕ is a transitive right group action of \mathbf{G}_{ES} on \mathcal{M} .

Theorem 4 Define the map $\Lambda : \mathcal{M} \times \mathbb{L} \rightarrow \mathfrak{ges}$ by

$$\Lambda(\xi, u) := (\Lambda_1(\xi, u), \Lambda_2(\xi, u)),$$

where $\Lambda_1 : \mathcal{M} \times \mathbb{L} \rightarrow \mathfrak{se}_2(3)$, and $\Lambda_2 : \mathcal{M} \times \mathbb{L} \rightarrow \mathbb{R}^6$ are given by

$$\Lambda_1(\xi, u) := (\mathbf{W} - \mathbf{B} + \mathbf{D}) + \mathbf{T}^{-1}(\mathbf{G} - \mathbf{D})\mathbf{T}, \quad (12)$$

$$\Lambda_2(\xi, u) := \boldsymbol{\tau}. \quad (13)$$

Then, Λ is a lift for the system in Equ. (10) with respect to the symmetry group $\mathbf{G}_{\text{ES}} := \mathbf{SE}_2(3) \times \mathbb{R}^6$.

Applying the EqF filter design methodology to this symmetry leads to the Imperfect-IEKF [1, 2]. Note that ignoring the bias and considering only the navigation states is the original IEKF filter [1]. The imperfect term comes from breaking the group-affine symmetry of the navigation states by adding the direct product terms for the bias.

4.3 Two-Frame group: $\mathbf{G}_{\text{TF}} : \mathbf{SO}(3) \times (\mathbb{R}^6 \oplus \mathbb{R}^6)$

The recently published two-frame group invariant extended Kalman filter [3] is one approach to address the theoretical issue in the imperfect IEKF for INS where the bias terms are not part of the symmetry structure.

Consider the system in Equ. (10). Define the symmetry group $\mathbf{G}_{\text{TF}} := \mathbf{SO}(3) \times (\mathbb{R}^6 \oplus \mathbb{R}^6)$, where $\mathbf{SO}(3)$ acts on two vector spaces of 6 dimensions each defined with respect to two different frames of references. Let $X = (C, \gamma) \in \mathbf{G}_{\text{TF}}$, with $C = (A, (a, b)) \in \mathbf{SE}_2(3) := \mathbf{SO}(3) \times \mathbb{R}^6$ such that $A \in \mathbf{SO}(3)$, $(a, b) \in \mathbb{R}^6$. Let, $*$: $\mathbf{SO}(3) \times \mathbb{R}^{3N} \rightarrow \mathbb{R}^{3N}$ be the rotation term introduced in [3], such that $\forall A \in \mathbf{SO}(3)$ and $x = (x_1, \dots, x_N) \in \mathbb{R}^{3N}$, $A * x = (Ax_1, \dots, Ax_N)$. Define the group product $XY = (C_X C_Y, \gamma_X + \text{Ad}_{C_X}[\gamma_Y])$. The inverse element of the symmetry group writes $X^{-1} = (C^{-1}, -A^T * \gamma) \in \mathbf{G}_{\text{TF}}$.

Lemma 5 Define $\phi : \mathbf{G}_{\text{TF}} \times \mathcal{M} \rightarrow \mathcal{M}$ as

$$\phi(X, \xi) := (\mathbf{TC}, A^T * (\mathbf{b} - \gamma)) \in \mathcal{M}. \quad (14)$$

Then, ϕ is a transitive right group action of \mathbf{G}_{TF} on \mathcal{M} .

Theorem 6 Define $\Lambda_1 : \mathcal{M} \times \mathbb{L} \rightarrow \mathfrak{se}_2(3)$ as

$$\Lambda_1(\xi, u) := (\mathbf{W} - \mathbf{B} + \mathbf{D}) + \mathbf{T}^{-1}(\mathbf{G} - \mathbf{D})\mathbf{T}, \quad (15)$$

define $\Lambda_2 : \mathcal{M} \times \mathbb{L} \rightarrow \mathbb{R}^6$ as

$$\Lambda_2(\xi, u) := (\mathbf{b}_\omega^\wedge (\boldsymbol{\omega} - \mathbf{b}_\omega) - \boldsymbol{\tau}_\omega, \mathbf{b}_a^\wedge (\boldsymbol{\omega} - \mathbf{b}_\omega) - \boldsymbol{\tau}_a). \quad (16)$$

Then, the map $\Lambda(\xi, u) = (\Lambda_1(\xi, u), \Lambda_2(\xi, u), \Lambda_2(\xi, u))$ is a lift for the system in Equ. (10) with respect to the symmetry group $\mathbf{G}_{\text{TF}} := \mathbf{SO}(3) \times (\mathbb{R}^6 \oplus \mathbb{R}^6)$.

In the appendix, it is shown that designing an EqF based on this symmetry leads to the recently published TFG-IEKF [3].

4.4 Tangent group $\mathbf{G}_{\text{TG}} : \mathbf{SE}_2(3) \times \mathfrak{se}_2(3)$

Recent work [21, 20] considered symmetries and EqF filter design on the tangent group TG of a general Lie-group. Since bias states are closely related to velocities, these ideas can easily be extended symmetries for bias states [9].

Define $\xi = (\mathbf{T}, \mathbf{b}) \in \mathcal{M} := \mathcal{SE}_2(3) \times \mathbb{R}^9$ to be the state space of the system. $\mathbf{T} \in \mathcal{SE}_2(3)$ represents the extended pose, whereas $\mathbf{b} = (\mathbf{b}_\omega, \mathbf{b}_a, \mathbf{b}_\nu) \in \mathbb{R}^9$ represents the IMU biases, and an additional virtual bias \mathbf{b}_ν . Let $u = (\mathbf{w}, \boldsymbol{\tau}) \in \mathbb{L} \subseteq \mathbb{R}^{18}$ denote the system input, where $\mathbf{w} = (\boldsymbol{\omega}, \mathbf{a}, \boldsymbol{\nu}) \in \mathbb{R}^9$ denotes the input given by the IMU readings, and an additional virtual input $\boldsymbol{\nu}$. $\boldsymbol{\tau} = (\boldsymbol{\tau}_\omega, \boldsymbol{\tau}_a, \boldsymbol{\tau}_\nu) \in \mathbb{R}^9$ denotes the input for the IMU biases. Define the matrices

$$\begin{aligned} \mathbf{G} &= (\bar{\mathbf{g}})^\wedge \in \mathfrak{se}_2(3), \\ \mathbf{B} &= \mathbf{b}^\wedge \in \mathfrak{se}_2(3), \quad \mathbf{D} = \begin{bmatrix} \mathbf{0}_{3 \times 3} & \mathbf{0}_{3 \times 1} & \mathbf{0}_{3 \times 1} \\ \mathbf{0}_{1 \times 3} & 0 & 1 \\ \mathbf{0}_{1 \times 3} & 0 & 0 \end{bmatrix} \in \mathbb{R}^{5 \times 5}, \\ \mathbf{W} &= \mathbf{w}^\wedge \in \mathfrak{se}_2(3), \end{aligned}$$

With these newly defined matrices, the system in Equ. (1) may then be written in compact form as in Equ. (10).

Define the symmetry group $\mathbf{G}_{\text{TG}} := \mathbf{SE}_2(3) \times \mathfrak{se}_2(3)$, and let $X = (C, \gamma) \in \mathbf{G}_{\text{TG}}$, where $C \in \mathbf{SE}_2(3)$, $\gamma \in \mathfrak{se}_2(3)$. Let $X = (C_X, \gamma_X)$, $Y = (C_Y, \gamma_Y)$ be two elements of the symmetry group, then the group product is written $XY = (C_X C_Y, \gamma_X + \text{Ad}_{C_X}[\gamma_Y])$. The inverse of an element X is given by $X^{-1} = (C^{-1}, -\text{Ad}_{C^{-1}}[\gamma])$.

Lemma 7 Define $\phi : \mathbf{G}_{\text{TG}} \times \mathcal{M} \rightarrow \mathcal{M}$ as

$$\phi(X, \xi) := (\mathbf{TC}, \text{Ad}_{C^{-1}}^\vee(\mathbf{b} - \gamma^\vee)) \in \mathcal{M}. \quad (17)$$

Then, ϕ is a transitive right group action of \mathbf{G}_{TG} on \mathcal{M} .

From here, we derive a compatible action of the symmetry group \mathbf{G}_{TG} on the input space \mathbb{L} and derive the lift Λ via constructive design as described in [15, 24].

Lemma 8 Define $\psi : \mathbf{G}_{\text{TG}} \times \mathbb{L} \rightarrow \mathbb{L}$ as

$$\psi(X, u) := (\text{Ad}_{C^{-1}}^\vee(\mathbf{w} - \gamma^\vee) + \Omega^\vee(C^{-1}), \text{Ad}_{C^{-1}}^\vee \boldsymbol{\tau}) \in \mathbb{L}. \quad (18)$$

Then, ψ is a right group action of \mathbf{G}_{TG} on \mathbb{L} .

The system in Equ. (10) is equivariant under the actions ϕ in Equ. (17) and ψ in Equ. (18). The existence of a

transitive group action of the symmetry group $\mathbf{G}_{\mathbf{T}\mathbf{G}}$ on the state space \mathcal{M} and the equivariance of the system guarantees the existence of an equivariant lift [15].

Theorem 9 Define the map $\Lambda : \mathcal{M} \times \mathbb{L} \rightarrow \mathfrak{g}_{\mathbf{T}\mathbf{G}}$ by

$$\Lambda(\xi, u) := (\Lambda_1(\xi, u), \Lambda_2(\xi, u)),$$

where $\Lambda_1 : \mathcal{M} \times \mathbb{L} \rightarrow \mathfrak{se}_2(3)$, and $\Lambda_2 : \mathcal{M} \times \mathbb{L} \rightarrow \mathfrak{se}_2(3)$ are given by

$$\Lambda_1(\xi, u) := (\mathbf{W} - \mathbf{B} + \mathbf{D}) + \mathbf{T}^{-1}(\mathbf{G} - \mathbf{D})\mathbf{T}, \quad (19)$$

$$\Lambda_2(\xi, u) := \text{ad}_{\mathbf{b}}[\Lambda_1(\xi, u)] - \boldsymbol{\tau}^\wedge. \quad (20)$$

Then, Λ is an equivariant lift for the system in Equ. (10) with respect to the symmetry group $\mathbf{G}_{\mathbf{T}\mathbf{G}} := \mathbf{SE}_2(3) \times \mathfrak{se}_2(3)$.

This approach requires the introduction of a new state \mathbf{b}_ν in order to apply the full $\mathfrak{se}_2(3)$ semi-direct symmetry on the bias states. This new state is entirely virtual, it does not exist in the real system. Since introducing an entirely virtual state just for the sake of the symmetry appears questionable, it is of interest to consider alternative symmetries that try to preserve the semi-direct group structure that models bias interaction, but doesn't require the additional bias filter state.

4.5 Direct Position group $\mathbf{G}_{\mathbf{D}\mathbf{P}} : \mathbf{HG}(3) \times \mathfrak{hg}(3) \times \mathbb{R}^3$

In this subsection, we define a symmetry to accomplish two goals simultaneously. First, we aim for a symmetry that does not require the over-parametrization of the state introduced in [9] given by the addition of a velocity bias state, and second, we aim for a symmetry with linear output for position measurements.

We introduce the term $\mathbf{HG}(3)$ for the *homogeneous Galilean* group. This corresponds to extended pose transformations $\mathbf{SE}_2(3)$ where the spatial translation is zero. That is the symmetry acts on rotation and velocity only with the semi-direct product induced by the $\mathbf{SE}_2(3)$ geometry. The homogeneous Galilean group is isomorphic to $\mathbf{SE}(3)$ in structure, however, since $\mathbf{SE}(3)$ is synonymous with pose transformation we use the $\mathbf{HG}(3)$ notation to avoid confusion.

The first step towards these goals is to introduce a virtual input $\boldsymbol{\nu}$ and rewrite Equ. (1c) as $\dot{\mathbf{p}} = \mathbf{R}\boldsymbol{\nu} + \mathbf{v}$.

Define $\xi = (\mathbf{T}, \mathbf{p}, \mathbf{b}) \in \mathcal{M} := \mathcal{HG}(3) \times \mathbb{R}^3 \times \mathbb{R}^6$ to be the state space of the system, where $\mathbf{T} = (\mathbf{R}, \mathbf{v}) \in \mathcal{HG}(3)$ includes the orientation and the velocity of the rigid body. Let $u = (\mathbf{w}, \boldsymbol{\nu}, \boldsymbol{\tau}) \in \mathbb{L} \subseteq \mathbb{R}^{15}$ denote the system input. Define the matrices

$$\mathbf{G} = (\bar{\mathbf{g}})^\wedge \in \mathfrak{se}(3), \quad \mathbf{B} = \mathbf{b}^\wedge \in \mathfrak{se}(3), \quad \mathbf{W} = \mathbf{w}^\wedge \in \mathfrak{se}(3).$$

Then, the system in Equ. (1) may then be written as

$$\dot{\mathbf{T}} = \mathbf{T}(\mathbf{W} - \mathbf{B}) + \mathbf{G}\mathbf{T}, \quad (21a)$$

$$\dot{\mathbf{p}} = \mathbf{R}\boldsymbol{\nu} + \mathbf{v}, \quad (21b)$$

$$\dot{\mathbf{b}} = \boldsymbol{\tau}. \quad (21c)$$

Define the symmetry group $\mathbf{G}_{\mathbf{D}\mathbf{P}} := \mathbf{HG}(3) \times \mathfrak{se}(3) \times \mathbb{R}^3$, and let $X = (B, \beta, c) \in \mathbf{G}_{\mathbf{D}\mathbf{P}}$ with $B = (A, a) \in \mathbf{HG}(3)$ such that $A \in \mathbf{SO}(3)$, $a \in \mathbb{R}^3$. Let $X = (B_X, \beta_X, c_X), Y = (B_Y, \beta_Y, c_Y) \in \mathbf{G}_{\mathbf{D}\mathbf{P}}$, the group product is written $XY = (B_X B_Y, \beta_X + \text{Ad}_{B_X}[\beta_Y], c_X + c_Y)$. The inverse of an element $X \in \mathbf{G}_{\mathbf{D}\mathbf{P}}$ is given by $X^{-1} = (B^{-1}, -\text{Ad}_{B^{-1}}[\beta], -c) \in \mathbf{G}_{\mathbf{D}\mathbf{P}}$.

Lemma 10 Define $\phi : \mathbf{G}_{\mathbf{D}\mathbf{P}} \times \mathcal{M} \rightarrow \mathcal{M}$ as

$$\phi(X, \xi) := (\mathbf{T}B, \text{Ad}_{B^{-1}}^\vee(\mathbf{b} - \beta^\vee), \mathbf{p} + c) \in \mathcal{M}. \quad (22)$$

Then, ϕ is a transitive right group action of $\mathbf{G}_{\mathbf{D}\mathbf{P}}$ on \mathcal{M} .

We derive a compatible action of the symmetry group $\mathbf{G}_{\mathbf{D}\mathbf{P}}$ on the input space \mathbb{L} .

Lemma 11 Define $\psi : \mathbf{G}_{\mathbf{D}\mathbf{P}} \times \mathbb{L} \rightarrow \mathbb{L}$ as

$$\psi(X, u) := (\text{Ad}_{B^{-1}}^\vee(\mathbf{w} - \beta^\vee), A^T(\boldsymbol{\nu} - a), \text{Ad}_{B^{-1}}^\vee \boldsymbol{\tau}) \in \mathbb{L}. \quad (23)$$

Then, ψ is a right group action of $\mathbf{G}_{\mathbf{D}\mathbf{P}}$ on \mathbb{L} .

The system in Equ. (21) is equivariant under the actions ϕ in Equ. (22) and ψ in Equ. (23). Therefore, the existence of an equivariant lift is guaranteed.

Theorem 12 Define the map $\Lambda : \mathcal{M} \times \mathbb{L} \rightarrow \mathfrak{g}_{\mathbf{D}\mathbf{P}}$ by

$$\Lambda(\xi, u) := (\Lambda_1(\xi, u), \Lambda_2(\xi, u), \Lambda_3(\xi, u)),$$

where $\Lambda_1 : \mathcal{M} \times \mathbb{L} \rightarrow \mathfrak{hg}(3)$, $\Lambda_2 : \mathcal{M} \times \mathbb{L} \rightarrow \mathfrak{se}(3)$, and $\Lambda_3 : \mathcal{M} \times \mathbb{L} \rightarrow \mathbb{R}^3$ are given by

$$\Lambda_1(\xi, u) := (\mathbf{W} - \mathbf{B}) + \mathbf{T}^{-1}\mathbf{G}\mathbf{T}, \quad (24)$$

$$\Lambda_2(\xi, u) := \text{ad}_{\mathbf{b}^\wedge}[\Lambda_1(\xi, u)] - \boldsymbol{\tau}^\wedge, \quad (25)$$

$$\Lambda_3(\xi, u) := \mathbf{R}\boldsymbol{\nu} + \mathbf{v}. \quad (26)$$

Then, the Λ is an equivariant lift for the system in Equ. (21) with respect to the symmetry group $\mathbf{G}_{\mathbf{D}\mathbf{P}} := \mathbf{HG}(3) \times \mathfrak{hg}(3) \times \mathbb{R}^3$.

The symmetry proposed in this subsection allows for linear position measurements, while keeping a minimal state parametrization (i.e. absence of over-parametrization of the state with additional state variables in the). However, the construction comes at the cost of separating the position state from the geometric $\mathbf{SE}_2(3)$ structure and modelling it as a direct product linear space.

4.6 Semi-Direct Bias group: $\mathbf{G}_{\text{SD}} : \mathbf{SE}_2(3) \ltimes \mathfrak{se}(3)$

In this subsection, we propose a symmetry that maintains a minimal state representation (not requiring the introduction of an additional velocity bias state) and keeps the position state within the geometric structure given by $\mathbf{SE}_2(3)$, leading hopefully to better linearization of the error dynamics.

Consider the system in Equ. (10). Define the symmetry group $\mathbf{G}_{\text{SD}} := \mathbf{SE}_2(3) \ltimes \mathfrak{se}(3)$ with group product $XY = (C_X C_Y, \gamma_X + \text{Ad}_{C_X} [\gamma_Y])$ for $X = (C_X, \gamma_X), Y = (C_Y, \gamma_Y) \in \mathbf{G}_{\text{SD}}$. Here, for $X = (C, \gamma) \in \mathbf{G}_{\text{SD}}$ one has $C = (A, a, b) = (B, b) \in \mathbf{SE}_2(3)$ such that $A \in \mathbf{SO}(3)$, $a, b \in \mathbb{R}^3$, and $B = (A, a) \in \mathbf{HG}(3)$. The element $C \in \mathbf{SE}_2(3)$ in its matrix representation is written

$$C = \begin{bmatrix} A & a & \vdots & b \\ \mathbf{0}_{1 \times 3} & 1 & \vdots & 0 \\ \dots & \dots & \dots & \dots \\ \mathbf{0}_{1 \times 3} & 0 & \vdots & 1 \end{bmatrix} = \begin{bmatrix} & & & b \\ & & & 0 \\ \dots & & & \dots \\ \mathbf{0}_{1 \times 3} & 0 & \vdots & 1 \end{bmatrix} \in \mathbf{SE}_2(3).$$

The inverse element is written

$$X^{-1} = (C^{-1}, -\text{Ad}_{B^{-1}} [\gamma]) \in \mathbf{G}_{\text{SD}}.$$

Lemma 13 Define $\phi : \mathbf{G}_{\text{SD}} \times \mathcal{M} \rightarrow \mathcal{M}$ as

$$\phi(X, \xi) := (\mathbf{T}C, \text{Ad}_{B^{-1}}^\vee (b - \gamma^\vee)) \in \mathcal{M}. \quad (27)$$

Then, ϕ is a transitive right group action of \mathbf{G}_{SD} on \mathcal{M} .

Theorem 14 Define $\Lambda_1 : \mathcal{M} \times \mathbb{L} \rightarrow \mathfrak{se}_2(3)$ as

$$\Lambda_1(\xi, u) := (\mathbf{W} - \mathbf{B} + \mathbf{D}) + \mathbf{T}^{-1}(\mathbf{G} - \mathbf{D})\mathbf{T}, \quad (28)$$

define $\Lambda_2 : \mathcal{M} \times \mathbb{L} \rightarrow \mathfrak{se}(3)$ as

$$\Lambda_2(\xi, u) := \text{ad}_{b^\vee} [\Pi(\Lambda_1(\xi, u))] - \tau^\wedge, \quad (29)$$

Then, the map $\Lambda(\xi, u) = (\Lambda_1(\xi, u), \Lambda_2(\xi, u))$ is a lift for the system in Equ. (10) with respect to the symmetry group $\mathbf{G}_{\text{SD}} := \mathbf{SE}_2(3) \ltimes \mathfrak{se}(3)$.

The symmetry proposed in this subsection is a variation of the symmetry defined in our previous work [9] that does not require over-parametrization of the state and additional state variables. Comparing to the DP-EqF structure, the position measurements of the SD-EqF are not globally linear and this may impact on performance for certain transient conditions.

5 Reformulation of Position Measurements as Equivariant

It is straightforward to verify the $\mathbf{G}_{\text{ES}}, \mathbf{G}_{\text{TG}}, \mathbf{G}_{\text{SD}}, \mathbf{G}_{\text{TF}}$ symmetries do not possess output equivariance [24, 25]

for global position measurements directly. In the present section, we show how position measurements can be reformulated as relative body-frame measurements imposing a nonlinear constraint [11]. Using this trick, the modified measurement is output equivariant with respect to a suitable group action, and the linearization methodology proposed in [25] can be applied to generate cubic linearization error in the output.

Lemma 15 Let π be a measurement of global position. Define a new measurement model $h(\xi) \in \mathbb{R}^3$, describing the body-referenced difference between the measured global position and the position state as follows

$$h(\xi) = \mathbf{R}^T (\pi - \mathbf{p}) \in \mathbb{R}^3. \quad (30)$$

Let $y = h(\xi) \in \mathcal{N}$ be a measurement defined according to the above model in Equ. (30), define $\rho : \mathbf{G} \times \mathbb{R}^3 \rightarrow \mathbb{R}^3$ as

$$\rho(X, y) := A^T (y - b). \quad (31)$$

Then, the configuration output defined in Equ. (30) is equivariant.

The noise-free value for y is zero and the output innovation $\delta(\rho_{\hat{X}^{-1}}(\mathbf{0})) = \rho_{\hat{X}^{-1}}(\mathbf{0}) - \pi$ measures the mismatch of the observer state in reconstructing the true state up to noise in the raw measurement π .

6 Linearization Error Analysis and EqF Design

In Sec. 4, we present different symmetry groups for the inertial navigation problem. An indicator of the performance of an EqF with a particular symmetry is the order of approximation error in the associated linearization of error dynamics.

For all symmetries, the origin $\xi \in \mathcal{M}$ is chosen to be $\xi := (\mathring{\mathbf{R}}, \mathring{\mathbf{v}}, \mathring{\mathbf{p}}, \mathring{\mathbf{b}}_\omega, \mathring{\mathbf{b}}_a) = (\mathbf{I}_3, \mathbf{0}_{3 \times 1}, \mathbf{0}_{3 \times 1}, \mathbf{0}_{3 \times 1}, \mathbf{0}_{3 \times 1})$. Define the local coordinate chart $\vartheta : \mathcal{U}_\xi \rightarrow \mathbb{R}^n$, to be

$$\vartheta := (\phi_\xi \cdot \exp_{\mathbf{G}})^{-1} = \log_{\mathbf{G}} \cdot \phi_\xi^{-1}, \quad (32)$$

on a neighborhood of $\xi \in \mathcal{M}$ such that $\log_{\mathbf{G}} \cdot \phi_\xi^{-1}$ is bijective. The chart ϑ is always well-defined locally since all group actions considered are free. The local error coordinates are defined by $\varepsilon := \vartheta(e)$, so long as $e := \phi(\hat{X}^{-1}, \xi)$ remains in the domain of definition of ϑ .

In Equ. (32), $\log_{\mathbf{G}}$ denotes the log coordinates on the symmetry group considered. This map is different for each symmetry group. For a product Lie group $\mathbf{G} := \mathbf{G}_1 \times \mathbf{G}_2$, the logarithm is given by $\log_{\mathbf{G}}((A, B)) = (\log_{\mathbf{G}_1}(A), \log_{\mathbf{G}_2}(B))$. When the product groups are Lie groups with well-known exponential maps, then the standard expressions are used [7]. For the semi-direct product groups $\mathbf{G} \ltimes \mathfrak{g}$ where \mathfrak{g} is the Lie algebra of \mathbf{G} , we

will use a matrix realization to compute the exponential algebraically.

In Tab. 2, we present the linearization of the state error dynamics associated with each of the symmetries considered. The linearization is expressed in terms of elements $\varepsilon = \log(E) \in \mathfrak{g}$ where the element $E \in \mathbf{G}$ corresponds bijectively to the error $e \in \mathcal{M}$ through the free group action. That is, we solve

$$D\vartheta^{-1}(\varepsilon)[\dot{\varepsilon}] \approx \frac{d}{dt}e = \tilde{f}(\vartheta^{-1}(\varepsilon), u)$$

for $\dot{\varepsilon}$ to first order in ε . Here $\dot{e} = \tilde{f}(e, u)$ is the full error dynamics expressed as a function of e and the input u [17, 25]. Finally, the filter design follows the procedure outlined in the authors’ earlier works [25, 18, 9, 8]. The detailed derivation of the error linearization for each symmetry, as well as the related equivariant filters, are provided in the appendix.

Barrau and Bonnabel [1] developed the IEKF for the bias free INS problem and showed that the linearization of the navigation states was exact. This was a significant improvement on the MEKF geometry, where the linearization of the navigation states is not exact, independently of the bias. However, this exact linearization property is lost when bias is added to the INS problem, the system is no longer group affine [2]. Using a direct product geometric structure to add bias leads to the Imperfect-IEKF [2] and introduces linearization error in the navigation state equations (cf. Tab. 2). The remaining filters all model coupling between bias and navigation states using semi-direct geometry of some form or other. The TG-EqF is the only filter for which the linearization of the navigation state is exact. In this case, the linearization error is only present in the bias states. The DP-EqF, SD-EqF and TFG-IEKF all have semi-direct geometric coupling between part of their navigation states and the bias states leading to exact or improved linearization where the coupling acts compatibly with the TG structure.

7 Experiments

In the present section, we document results from a suite of experiments chosen to provide a comparison of the performance of the MEKF, the Imperfect-IEKF, the TFG-IEKF, an EqF based on the $\mathbf{G}_{\mathbf{TG}}$ symmetry [9] termed TG-EqF, an EqF based on the $\mathbf{G}_{\mathbf{DP}}$ symmetry termed DP-EqF, an EqF based on the $\mathbf{G}_{\mathbf{SD}}$ symmetry termed SD-EqF, and finally an implementation of the TFG-IEKF in [3] (implemented according to the author’s original manuscript, and verified to behave the same as an EqF based on the $\mathbf{G}_{\mathbf{TF}}$ symmetry). We undertake two separate experimental analyses. In the first experiment, we undertake a Monte-Carlo simulation of an unmanned aerial vehicle (UAV) equipped with an

Table 3
ANEES in the first half (transient (T)) and the second half (asymptotic (A)) of the trajectory length.

Filter	ANEES (T)	ANEES (A)
MEKF	3.11	1.69
Imperfect-IEKF	1.36	1.40
TFG-IEKF	1.71	1.43
TG-EqF	1.20	1.22
DP-EqF	1.44	1.42
SD-EqF	1.32	1.44

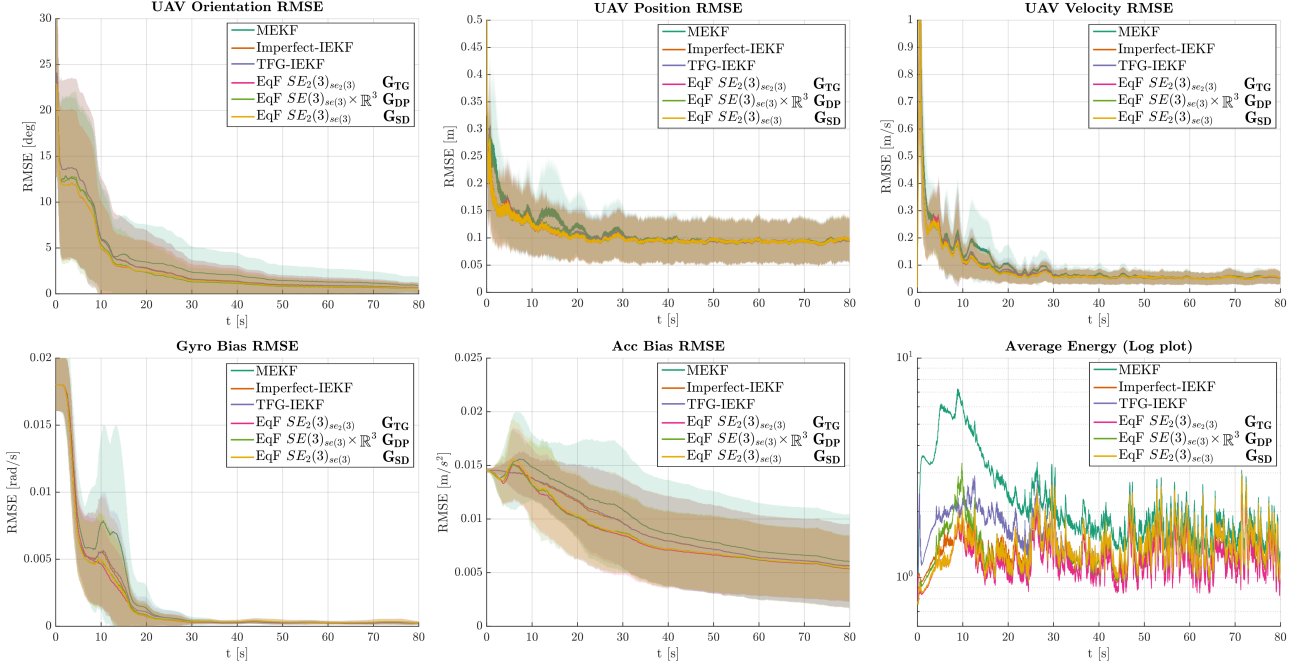
IMU receiving acceleration and angular velocity measurements at 200Hz and receiving global position measurements at 10Hz, simulating a GNSS receiver. In the second experiment, we compare all the filters with real data from the INSANE dataset [4].

7.1 UAV Flight Simulation

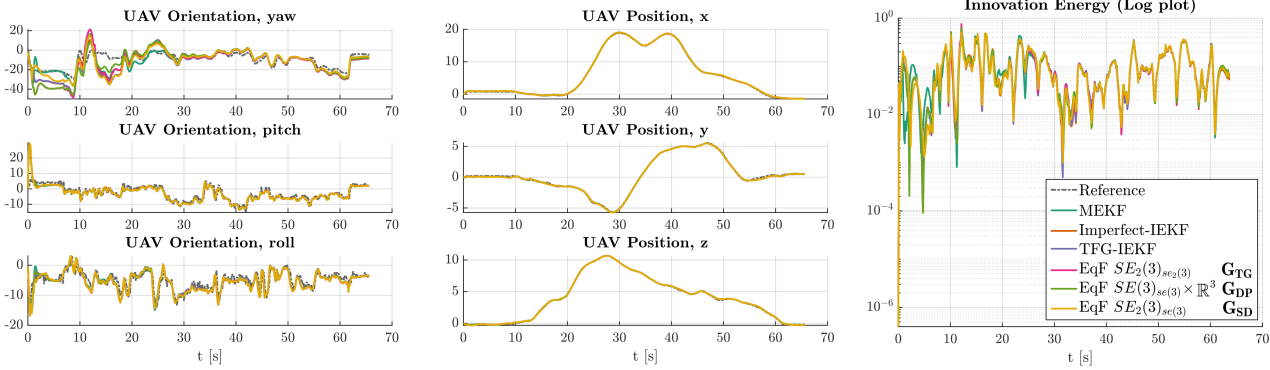
In this experiment, we conducted a Monte-Carlo simulation, including four hundred runs of a simulated UAV equipped with an IMU and receiving global position measurements simulating a GNSS receiver. In order to simulate realistic flight conditions, we selected the initial 80s from four sequences in the Euroc dataset’s vicon room [6] as reference trajectories. For each sequence, we generated a hundred runs, incorporating synthetic IMU data and position measurements while varying the initial conditions for the position (distributed normally around zero with 1m standard deviation per axis) and the attitude (distributed normally around zero with 20° standard deviation per axis).

The ground truth IMU biases are randomly generated every run following a Gaussian distribution with standard deviation of $0.01\text{rad/s}\sqrt{s}$ for the gyro bias and $0.01\text{m/s}^2\sqrt{s}$ for the accelerometer bias. To simulate realistic global position measurement, additive Gaussian noise with a standard deviation of 0.2m per axis is added.

For a fair comparison, we were careful to use the same prior distributions and noise parameters for all filters. This includes accounting for the different scaling and transformations of noise due to the input and state parametrizations for the different geometries. Similarly, each filter shares the same input and output measurement noise covariance adapted to the particular geometry of the filter. The validity of the noise models can be verified in the Average Energy plot (Fig. 1a), which plots the average normalized estimation error squared (ANEES) [13]. Here, all filters initialize with unity ANEES, demonstrating that the prior sampling and observer response corresponds to the stochastic prior used, and all filters converge towards unity ANEES as expected from a filter driven by Gaussian noise. All the filters are initialized at the identity (zero attitude, zero position, zero velocity, and zero biases).



(a) Average RMSE and sample variance (shaded) of the filters' states, and full filter energy.



(b) Orientation and position states evolution, and innovation energy for the real-world UAV flight experiment.

Figure 1. Simulation and real-world experiments' results. Orange: Imperfect-IEKF. Purple: TFG-IEKF. Magenta: TG-EqF. Green: DP-EqF. Yellow: SD-EqF.

The primary plots in Fig. 1a are RMSE plots for the navigation states (on the top) and the bias states (on the bottom). It is clear that the MEKF filter demonstrates worse performance than the modern geometric filters. There is little difference visible in the transient and asymptotic error response of the navigation states for the modern filters. The remaining attitude error is due to yaw error, which is poorly observable for this scenario. The position and velocity errors converge to the noise limits of the measurement signals. In contrast, there are clear differences visible in the transient response of the bias states. The filters split roughly into three categories: the three filters with semi-direct bias symmetry (TG-EqF, DP-EqF and SD-EqF) appear to display the best transient response in both gyrometer

and accelerometer bias. The TG-EqF appears slightly better in the gyrometer bias. The IEKF and TFG-IEKF, which have the $\mathbf{SE}_2(3)$ symmetry but do not use a semi-direct geometry for the bias geometry, have almost identical bias transient. The accelerometer bias, in particular, is clearly separated from the filters with the semi-direct group symmetry. Finally, the MEKF suffers from not modeling the $\mathbf{SE}_2(3)$ symmetry at all.

The average energy plot provides an additional important analysis tool. This plot shows the ANEES [13] defined as

$$\text{ANEES} = \frac{1}{nM} \sum_{i=1}^M \boldsymbol{\varepsilon}_i^T \boldsymbol{\Sigma}_i^{-1} \boldsymbol{\varepsilon}_i,$$

where $\boldsymbol{\varepsilon}$ is the specific filter error state, $\boldsymbol{\Sigma}$ is the error

covariance, $M = 400$ is the number of runs in the Monte-Carlo simulation, and n is the dimension of the state space. The ANEES provides a measure of the consistency of the filter estimate. An ANEES of unity means that the observed error variance corresponds exactly to the estimated covariance of the information state. When ANEES is larger than unity, it indicates that the filter is overconfident; that is, the observed error is larger than the estimate of the state covariance predicts. All ‘pure’ extended Kalman filters tend to be overconfident since their derivation ignores linearization errors in the model. The closer to an ANEES of unity that a filter manages is directly correlated to the consistency of the filter estimate and is usually linked to smaller linearization errors. To provide numeric results, we have averaged the ANEES values over the transient and asymptotic sections of the filter response and presented them in Tab. 3. Here, it is clear that the TG-EqF is superior, the four filters IEKF, TFG-IEKF, DP-EqF and SD-EqF are similar, and the MEKF is worst. The ANEES of the MEKF diverges to over seven before converging, corresponding to an overconfidence of a factor of seven standard deviations in the state error. Such a level of overconfidence is dangerous in a real-world scenario and may indeed lead to divergence of the filter estimate in certain situations. Note that in practice, overconfidence of a filter is avoided by inflating the process noise model covariance to account for linearization error in the model. A more consistent filter requires a smaller covariance inflation and has correspondingly more confidence in its model than a filter that is less consistent.

In conclusion, the \mathbf{G}_{TG} EqF exhibits the best convergence rate, particularly in orientation and IMU biases, as well as the best consistency of all the filters. We believe that this performance can be traced back to the coupling of the IMU bias with the navigation states that are inherent in the semi-direct product structure of the symmetry group \mathbf{G}_{TG} and the exact linearization of the navigation error dynamics (Tab. 2). Note that the bias states are poorly observable states and possess slow dynamics. Consequently, moving linearization error into these states heuristically appears better than leaving the linearization error in the main navigation states that are much more dynamic.

7.2 Real-world UAV flight

In this experiment, we compared the performance of the discussed filters in a real-world UAV flight scenario from the INSANE dataset [4]. In particular, in this experiment, a quadcopter is flying for 50m at a maximum height of 13m covering an area of roughly 200m², at a maximum speed of 3m/s. The UAV is receiving IMU measurements at 200Hz, as well as measurements from and RTK-GNSS receiver at 8Hz with an accuracy between 0.1m and 0.6m. The position and orientation reference has been obtained as described in [4] from raw

sensor measurements of two RTK-GNSS and a magnetometer.

Similar to the previous experiments, all the filters share the same tuning parameters.

Fig. 1b shows the evolution of each filter orientation and position estimates, as well as the innovation energy, commonly referred to as the Normalised Innovation Squared (NIS) error

$$\text{NIS} = \frac{1}{n} \mathbf{r}^T \mathbf{S}^{-1} \mathbf{r},$$

where \mathbf{r} is the specific measurement residual of dimension n computed via the output action ρ and \mathbf{S} is the innovation covariance. The results in Fig. 1b show that the high level conclusions from the simulations are confirmed on real data. There are slight differences between filters in the plotted results but due to the lack of accurate ground truth all that can be deduced is that all the filters provide high quality real-world INS solutions. This is not surprising since the MEKF is the industry standard and is known to perform well in practice and the more modern filters are expected to improve on this performance.

8 Conclusion

This study investigates inertial navigation system filter design from the perspective of symmetry. We establish a unifying framework, demonstrating that various modern INS filter variants can be interpreted as equivariant filters applied to distinct choices of symmetry, with the group structure being the only difference among those filter variants. With specific application to position measurements, we demonstrated that fixed-frame measurements can be reformulated as body-frame relative measurements. This allows one to exploit the equivariance of the output, ensuring third-order linearization error in the measurement equations.

We discussed and presented different symmetry groups acting on the state-space of the INS problem. Novel symmetries are introduced alongside analysis of similarities and differences in the context of filter design. Furthermore, we showed how different choices of symmetries lead to filters with different linearized error dynamics, and how the \mathbf{G}_{TG} symmetry yields exact linearization of the navigation error, shifting all the linearisation error into the bias state dynamics.

Comparative performance studies in simulation, and real-world of a vehicle equipped with an IMU and receiving position measurement from a GNSS receiver highlighted that any of the IEKF, TFG-IEKF, TG-EqF, DP-EqF, and SD-EqF are good candidates for high performance INS filter design with the TG-EqF demonstrating superior performance.

A Linearization Error and equivariant filter design with Different Symmetries

In this section, we explicitly derive the linearization error in the error dynamics and the related filter matrices of each filter presented in Tab. 2.

A.1 Logarithm map of semi-direct product group

As mentioned in Sec. 6, for the semi-direct product groups $\mathbf{G} \ltimes \mathfrak{g}$ where \mathfrak{g} is the Lie algebra of \mathbf{G} , we will use a matrix realization to compute the exponential algebraically. Define $X = (C, \gamma) \in \mathbf{G} \ltimes \mathfrak{g}$, then X has a matrix representation given by

$$X = \begin{bmatrix} \text{Ad}_C^\vee & \vdots & \gamma^\vee \\ \dots & \dots & \dots \\ \mathbf{0} & \vdots & 1 \end{bmatrix} \in \mathbb{R}^{(\dim \mathfrak{g}+1) \times (\dim \mathfrak{g}+1)}$$

The logarithm is then given by

$$\log_{\mathbf{G} \ltimes \mathfrak{g}}(X) = \begin{bmatrix} \text{ad}_{\log_{\mathbf{G}}(C)}^\vee & \vdots & J_l(\log_{\mathbf{G}}(C))^{-1} \gamma^\vee \\ \dots & \dots & \dots \\ \mathbf{0} & \vdots & 0 \end{bmatrix},$$

where $J_l(\log_{\mathbf{G}}(C))$ is the left Jacobian of $\log_{\mathbf{G}}(C)$,

$$J_l(\log_{\mathbf{G}}(C)) = \sum_{k=0}^{\infty} \frac{1}{(k+1)!} \text{ad}_{\log_{\mathbf{G}}(C)}^\vee{}^k.$$

A.2 Equivariant filter design

Let the state origin to be the identity of the state space, thus $\hat{\xi} = \text{id} \in \mathcal{G}$. Let $e := \phi_{\hat{X}^{-1}}(\xi)$ be the equivariant error, define local coordinates of the state space, thus a chart, and a chart $\vartheta : \mathcal{U}_{\hat{\xi}} \subset \mathcal{M} \rightarrow \mathbb{R}^m$, where $m = \dim(\mathcal{M})$ is the dimension of the state space. Let $\hat{y} = h(\hat{\xi})$ be the output origin, then define local coordinates of the output space, thus a chart, and a chart $\delta : \mathcal{U}_{\hat{y}} \subset \mathcal{N} \rightarrow \mathbb{R}^n$, where $n = \dim(\mathcal{N})$ is the dimension of the output space.

Let ϵ denote the linearization of the error e in the chart ϑ . The linearized error dynamics, and the linearized output, are defined according to [24]

$$\begin{aligned} \dot{\epsilon} &\approx \mathbf{A}_t^0 \epsilon - D_e|_{\hat{\xi}} \vartheta(e) D_E|_I \phi_{\hat{\xi}}(E) [\Delta], \\ \mathbf{A}_t^0 &= D_e|_{\hat{\xi}} \vartheta(e) D_E|_I \phi_{\hat{\xi}}(E) D_e|_{\hat{\xi}} \Lambda(e, \hat{u}) D_\epsilon|_{\mathbf{0}} \vartheta^{-1}(\epsilon), \\ \delta(h(\xi)) - \delta(h(\hat{\xi})) &\approx \mathbf{C}^0 \epsilon, \\ \mathbf{C}^0 &= D_y|_{\hat{y}} \delta(y) D_e|_{\hat{\xi}} h(e) D_\epsilon|_{\mathbf{0}} \vartheta^{-1}(\epsilon). \end{aligned}$$

If no compatible action ψ of the symmetry group on the input space is found, the state matrix can be computed alternatively according to

$$\begin{aligned} \mathbf{A}_t^0 &= D_e|_{\hat{\xi}} \vartheta(e) D_\xi|_{\hat{\xi}} \phi_{\hat{X}^{-1}}(\xi) D_E|_I \phi_{\hat{\xi}}(E) \\ &D_\xi|_{\phi_{\hat{X}}(\hat{\xi})} \Lambda(\xi, u) D_e|_{\hat{\xi}} \phi_{\hat{X}}(e) D_\epsilon|_{\mathbf{0}} \vartheta^{-1}(\epsilon). \end{aligned}$$

If the output is equivariant, thus if an action ρ of the symmetry group in the output space exists, then this can be exploited to derive a linearized output with third order error [25] as follows

$$\begin{aligned} \delta(h(e)) &= \delta(\rho_{\hat{X}^{-1}}(h(\xi))) \approx \mathbf{C}^* \epsilon + \mathbf{O}(\epsilon^3), \\ \mathbf{C}^* \epsilon &= \frac{1}{2} D_y|_{\hat{y}} \delta(y) (D_E|_I \rho_E(y) + D_E|_I \rho_E(\rho_{\hat{X}^{-1}}(0))) \epsilon^\wedge. \end{aligned}$$

A.3 MEKF linearization error and filter design

A.3.1 Overview

The state space is defined to be $\mathcal{M} := \mathcal{SO}(3) \times \mathbb{R}^3 \times \mathbb{R}^3 \times \mathbb{R}^3 \times \mathbb{R}^3$ with $\xi := (\mathbf{R}, \mathbf{v}, \mathbf{p}, \hat{\mathbf{b}}_\omega, \hat{\mathbf{b}}_a) \in \mathcal{M}$. Choose the origin to be $\hat{\xi} := (\mathbf{I}_3, \mathbf{0}_{3 \times 1}, \mathbf{0}_{3 \times 1}, \mathbf{0}_{3 \times 1}, \mathbf{0}_{3 \times 1}) \in \mathcal{M}$. The velocity input is given by $u := (\boldsymbol{\omega}, \mathbf{a}, \boldsymbol{\tau}_\omega, \boldsymbol{\tau}_a)$.

The symmetry group of MEKF is given by $\mathbf{G}_O := \mathbf{SO}(3) \times \mathbb{R}^{12}$. Define the filter state $\hat{X} = (\hat{A}, \hat{a}, \hat{b}, \hat{\alpha}, \hat{\beta}) \in \mathbf{G}_O$, where $\hat{A} \in \mathbf{SO}(3)$ and $\hat{a}, \hat{b}, \hat{\alpha}, \hat{\beta} \in \mathbb{R}^3$. The state estimate is given by

$$\hat{\xi} := \phi(\hat{X}, \hat{\xi}) = (\hat{A}, \hat{a}, \hat{b}, \hat{\alpha}, \hat{\beta}) = (\hat{\mathbf{R}}, \hat{\mathbf{v}}, \hat{\mathbf{p}}, \hat{\mathbf{b}}_\omega, \hat{\mathbf{b}}_a). \quad (\text{A.1})$$

The state error is defined as

$$\begin{aligned} e := \phi(\hat{X}^{-1}, \xi) &= (\mathbf{R} \hat{A}^\top, \mathbf{v} - \hat{a}, \mathbf{p} - \hat{b}, \mathbf{b}_\omega - \hat{\alpha}, \mathbf{b}_a - \hat{\beta}), \\ &= (\mathbf{R} \hat{\mathbf{R}}^\top, \mathbf{v} - \hat{\mathbf{v}}, \mathbf{p} - \hat{\mathbf{p}}, \mathbf{b}_\omega - \hat{\mathbf{b}}_\omega, \mathbf{b}_a - \hat{\mathbf{b}}_a). \end{aligned} \quad (\text{A.2})$$

A.3.2 Error dynamics

The error dynamics related to Equ. (A.2) for each state is given by

$$\begin{aligned}
\dot{e}_R &= \frac{d}{dt}(\mathbf{R} \hat{\mathbf{R}}^\top) \\
&= \mathbf{R}(\boldsymbol{\omega} - \mathbf{b}_\omega)^\wedge \hat{\mathbf{R}}^\top - \mathbf{R} \hat{\mathbf{R}}^\top \hat{\mathbf{R}}(\boldsymbol{\omega} - \hat{\mathbf{b}}_\omega)^\wedge \hat{\mathbf{R}}^\top \\
&= \mathbf{R}(\boldsymbol{\omega} - \mathbf{b}_\omega - \boldsymbol{\omega} + \hat{\mathbf{b}}_\omega)^\wedge \hat{\mathbf{R}}^\top \\
&= -e_R \hat{\mathbf{R}} e_{b_\omega}^\wedge \hat{\mathbf{R}}^\top \\
&= -e_R (\hat{\mathbf{R}} e_{b_\omega})^\wedge; \\
\dot{e}_v &= \frac{d}{dt}(\mathbf{v} - \hat{\mathbf{v}}) = \dot{\mathbf{v}} - \dot{\hat{\mathbf{v}}} \\
&= \mathbf{R}(\mathbf{a} - \mathbf{b}_a)^\wedge + \mathbf{g} - \hat{\mathbf{R}}(\mathbf{a} - \hat{\mathbf{b}}_a)^\wedge - \mathbf{g} \\
&= \mathbf{R}(\mathbf{a} - \mathbf{b}_a)^\wedge - \hat{\mathbf{R}}(\mathbf{a} - \hat{\mathbf{b}}_a)^\wedge \\
&= e_R \hat{\mathbf{R}}(\mathbf{a} - \mathbf{b}_a) - \hat{\mathbf{R}}(\mathbf{a} - \hat{\mathbf{b}}_a); \\
\dot{e}_p &= \frac{d}{dt}(\mathbf{p} - \hat{\mathbf{p}}) = \dot{\mathbf{p}} - \dot{\hat{\mathbf{p}}} \\
&= \mathbf{v} - \hat{\mathbf{v}} = e_v; \\
\dot{e}_b &= \frac{d}{dt}(\mathbf{b} - \hat{\mathbf{b}}) = \mathbf{0}.
\end{aligned}$$

The local coordinate chart $\varepsilon = \log_{\mathbf{G}_\mathbf{O}} \circ \phi_\xi^{-1}(e)$ for each state is given by

$$\begin{aligned}
\varepsilon_R &:= \log_{\mathbf{SO}(3)}(e_R)^\vee \in \mathbb{R}^3 \\
\varepsilon_{v,p,b_\omega,b_a} &:= e_{v,p,b_\omega,b_a} \in \mathbb{R}^3.
\end{aligned}$$

The linearization of $\dot{e}_R = \text{Dexp}(\varepsilon_R^\wedge)[\dot{\varepsilon}_R^\wedge]$ is given by

$$\begin{aligned}
e_R \frac{\mathbf{I} - \exp(-\text{ad}_{\varepsilon_R^\wedge})}{\text{ad}_{\varepsilon_R^\wedge}} \dot{\varepsilon}_R^\wedge &= -e_R (\hat{\mathbf{R}} \varepsilon_{b_\omega})^\wedge \\
(\mathbf{I} + \mathcal{O}(\varepsilon_R^\wedge)) \dot{\varepsilon}_R^\wedge &= (\hat{\mathbf{R}} \varepsilon_{b_\omega})^\wedge \\
\dot{\varepsilon}_R &= \hat{\mathbf{R}} \varepsilon_{b_\omega} + \mathcal{O}(\varepsilon_R^2).
\end{aligned}$$

The linearization of $\dot{e}_v = \dot{\varepsilon}_v$ is given by

$$\begin{aligned}
\dot{\varepsilon}_v &= e_R \hat{\mathbf{R}}(\mathbf{a} - \mathbf{b}_a) - \hat{\mathbf{R}}(\mathbf{a} - \hat{\mathbf{b}}_a) \\
&= (\mathbf{I} + \varepsilon_R^\wedge + \mathcal{O}(\varepsilon_R^2)) \hat{\mathbf{R}}(\mathbf{a} - \mathbf{b}_a) - \hat{\mathbf{R}}(\mathbf{a} - \hat{\mathbf{b}}_a) \\
&= \hat{\mathbf{R}}(\hat{\mathbf{b}}_a - \mathbf{b}_a) + \varepsilon_R^\wedge \hat{\mathbf{R}}(\mathbf{a} - \mathbf{b}_a) + \mathcal{O}(\varepsilon_R^2) \\
&= -\hat{\mathbf{R}} \varepsilon_{b_a} + \varepsilon_R^\wedge \hat{\mathbf{R}}(\mathbf{a} - \varepsilon_{b_a} - \hat{\mathbf{b}}_a) + \mathcal{O}(\varepsilon^2) \\
&= -\hat{\mathbf{R}} \varepsilon_{b_a} + \varepsilon_R^\wedge \hat{\mathbf{R}}(\mathbf{a} - \hat{\mathbf{b}}_a) - \varepsilon_R^\wedge \hat{\mathbf{R}} \varepsilon_{b_a} + \mathcal{O}(\varepsilon_R^2) \\
&= -(\hat{\mathbf{R}}(\mathbf{a} - \hat{\mathbf{b}}_a))^\wedge \varepsilon_R - \hat{\mathbf{R}} \varepsilon_{b_a} + \mathcal{O}(\varepsilon^2).
\end{aligned}$$

The linearization of $\dot{e}_p = \dot{\varepsilon}_p$ is given by

$$\dot{\varepsilon}_p = \varepsilon_v.$$

The linearization of $\dot{e}_b = \dot{\varepsilon}_b$ is given by $\dot{\varepsilon}_b = \mathbf{0}$.

A.3.3 Filter design

From the linearization error analysis, it is trivial to see that the linearized error state matrix $\mathbf{A}_t^0 | \dot{\varepsilon} \simeq \mathbf{A}_t^0 \varepsilon$ is written

$$\mathbf{A}_t^0 = \begin{bmatrix} \vdots & -\hat{\mathbf{R}} & \mathbf{0}_{3 \times 3} \\ \mathbf{1}_A & \mathbf{0}_{3 \times 3} & -\hat{\mathbf{R}} \\ \vdots & \mathbf{0}_{3 \times 3} & \mathbf{0}_{3 \times 3} \\ \vdots & \vdots & \vdots \\ \mathbf{0}_{6 \times 9} & \vdots & \mathbf{0}_{6 \times 6} \end{bmatrix} \in \mathbb{R}^{15 \times 15}, \quad (\text{A.3})$$

where

$$\mathbf{1}_A = \begin{bmatrix} \mathbf{0}_{3 \times 3} & \mathbf{0}_{3 \times 3} & \mathbf{0}_{3 \times 3} \\ -(\hat{\mathbf{R}}(\mathbf{a} - \hat{\mathbf{b}}_a))^\wedge & \mathbf{0}_{3 \times 3} & \mathbf{0}_{3 \times 3} \\ \mathbf{0}_{3 \times 3} & \mathbf{I}_3 & \mathbf{0}_{3 \times 3} \end{bmatrix} \in \mathbb{R}^{9 \times 9}.$$

Position measurements are linear with respect to the defined error; therefore, the output matrix \mathbf{C}^0 yields

$$\mathbf{C}^0 = \begin{bmatrix} \mathbf{0}_{3 \times 6} & \mathbf{I}_3 & \mathbf{0}_{3 \times 3} & \mathbf{0}_{3 \times 6} \end{bmatrix} \in \mathbb{R}^{3 \times 15}. \quad (\text{A.4})$$

It is straightforward to verify that the derived equivariant filter is equivalent to the well-known MEKF, and the EqF state matrix in Equ. (A.3) corresponds directly to the state matrix of the MEKF [23, Sec. 7]

A.4 Imperfect-IEKF

A.4.1 Overview

The state space is defined as $\mathcal{M} := \mathcal{SE}_2(3) \times \mathbb{R}^6$ with $\xi := (\mathbf{T}, \mathbf{b}) \in \mathcal{M}$. One has $\mathbf{T} = (\mathbf{R}, \mathbf{v}, \mathbf{p}) \in \mathcal{SE}_2(3)$ and $\mathbf{b} = (\mathbf{b}_\omega, \mathbf{b}_a) \in \mathbb{R}^6$. Choose the origin to be $\xi^\circ = (\mathbf{I}_5, \mathbf{0}_{6 \times 1}) \in \mathcal{M}$. The velocity input is given by $u := (\boldsymbol{\omega}, \mathbf{a}, \boldsymbol{\tau}_\omega, \boldsymbol{\tau}_a)$.

The symmetry group of Imperfect-IEKF is given by $\mathbf{G}_{\text{ES}} : \mathbf{SE}_2(3) \times \mathbb{R}^6$. Define the filter state $\hat{X} = (\hat{C}, \hat{\gamma}) \in \mathbf{G}_{\text{ES}}$ with $\hat{C} = (\hat{A}, \hat{a}, \hat{b}) \in \mathbf{SE}_2(3)$ and $\hat{\gamma} = (\hat{\gamma}_\omega, \hat{\gamma}_a) \in \mathbb{R}^6$. The state estimate is given by

$$\hat{\xi} := \phi(\hat{X}, \hat{\xi}) = (\hat{A}, \hat{\gamma}) = (\hat{\mathbf{T}}, \hat{\mathbf{b}}). \quad (\text{A.5})$$

The state error is defined as

$$\begin{aligned}
e &:= \phi(\hat{X}^{-1}, \xi) = (\mathbf{T} \hat{C}^{-1}, \mathbf{b} - \hat{\gamma}), \\
&= (\mathbf{T} \hat{\mathbf{T}}^{-1}, \mathbf{b} - \hat{\mathbf{b}}).
\end{aligned} \quad (\text{A.6})$$

A.4.2 Error dynamics

The error dynamics related to Equ. (A.6) for each state is given by

$$\begin{aligned}
\dot{e}_R &= -e_R(\hat{\mathbf{R}}e_{b_\omega})^\wedge \text{ (Derivation same as MEKF);} \\
\dot{e}_v &= \frac{d}{dt}(-\mathbf{R}\hat{\mathbf{R}}^\top + \mathbf{v}) = \frac{d}{dt}(-\mathbf{R}\hat{\mathbf{R}}^\top \hat{\mathbf{v}} + \mathbf{v}) \\
&= -\dot{e}_R \hat{\mathbf{v}} - e_R \dot{\hat{\mathbf{v}}} + \dot{\mathbf{v}} \\
&= e_R(\hat{\mathbf{R}}e_{b_\omega})^\wedge \hat{\mathbf{v}} - e_R \hat{\mathbf{R}}(\mathbf{a} - \hat{\mathbf{b}}_a) - e_R \mathbf{g} + \mathbf{R}(\mathbf{a} - \mathbf{b}_a) + \mathbf{g} \\
&= e_R(\hat{\mathbf{R}}e_{b_\omega})^\wedge \hat{\mathbf{v}} - e_R \hat{\mathbf{R}}(\mathbf{a} - \hat{\mathbf{b}}_a) - e_R \mathbf{g} \\
&\quad + e_R \hat{\mathbf{R}}(\mathbf{a} - e_{b_a} + \hat{\mathbf{b}}_a) + \mathbf{g}; \\
\dot{e}_p &= \frac{d}{dt}(-\mathbf{R}\hat{\mathbf{R}}^\top \hat{\mathbf{p}} + \mathbf{p}) \\
&= -\dot{e}_R \hat{\mathbf{p}} - e_R \dot{\hat{\mathbf{p}}} + \dot{\mathbf{p}} \\
&= e_R(\hat{\mathbf{R}}e_{b_\omega})^\wedge \hat{\mathbf{p}} - e_R \hat{\mathbf{v}} + \mathbf{v} \\
&= e_R(\hat{\mathbf{R}}e_{b_\omega})^\wedge \hat{\mathbf{p}} + e_v; \\
\dot{e}_b &= \mathbf{0}.
\end{aligned}$$

The local coordinate chart $\varepsilon = \log_{\mathbf{G}_{\text{ES}}} \circ \phi_\xi^{-1}(e)$ for each state is given by

$$\begin{aligned}
\varepsilon_T &:= \log_{\mathbf{SE}_2(3)}(\phi_\xi^{-1}(e_T))^\vee = \log_{\mathbf{SE}_2(3)}(e_T)^\vee \in \mathbb{R}^9 \\
\varepsilon_{b_\omega, b_a} &:= e_{b_\omega, b_a} \in \mathbb{R}^3.
\end{aligned}$$

The linearization of \dot{e}_R is the same as the derivation in MEKF, given by

$$\dot{e}_R = \hat{\mathbf{R}}\varepsilon_{b_\omega} + O(\varepsilon_R^2).$$

The linearization of $\dot{e}_v = \dot{e}_v + O(\varepsilon^2)$ is given by

$$\begin{aligned}
\dot{e}_v &= -(I + \varepsilon_R^\wedge + O(\varepsilon_R^2))(\hat{\mathbf{R}}\varepsilon_{b_\omega})^\wedge \hat{\mathbf{v}} \\
&\quad - (I + \varepsilon_R^\wedge + O(\varepsilon_R^2))\hat{\mathbf{R}}(\mathbf{a} - \hat{\mathbf{b}}_a) \\
&\quad - (I + \varepsilon_R^\wedge + O(\varepsilon_R^2))\mathbf{g} \\
&\quad + (I + \varepsilon_R^\wedge + O(\varepsilon_R^2))\hat{\mathbf{R}}(\mathbf{a} - \varepsilon_{b_a} + \hat{\mathbf{b}}_a) \\
&\quad + \mathbf{g} + O(\varepsilon^2) \\
&= -\hat{\mathbf{v}}^\wedge \hat{\mathbf{R}}\varepsilon_{b_\omega} - \hat{\mathbf{R}}\varepsilon_{b_a} + \mathbf{g}^\wedge \varepsilon_R + O(\varepsilon^2).
\end{aligned}$$

The linearization of $\dot{e}_p = \dot{e}_p + O(\varepsilon^2)$ is given by

$$\begin{aligned}
\dot{e}_p &= (I + \varepsilon_R^\wedge + O(\varepsilon_R^2))(\hat{\mathbf{R}}e_{b_\omega})^\wedge \hat{\mathbf{p}} + \varepsilon_v + O(\varepsilon^2) \\
&= \varepsilon_v - \hat{\mathbf{p}}^\wedge \varepsilon_{b_\omega} + O(\varepsilon^2).
\end{aligned}$$

The linearization of $\dot{e}_b = \dot{e}_b$ is given by $\dot{e}_b = \mathbf{0}$.

A.4.3 Filter design

The linearized error state matrix $\mathbf{A}_t^0 \mid \dot{e} \simeq \mathbf{A}_t^0 \varepsilon$ yields

$$\mathbf{A}_t^0 = \begin{bmatrix} \vdots & -\hat{\mathbf{R}} & \mathbf{0}_{3 \times 3} \\ \mathbf{2A} & -\hat{\mathbf{v}}^\wedge \hat{\mathbf{R}} & -\hat{\mathbf{R}} \\ \vdots & -\hat{\mathbf{p}}^\wedge \hat{\mathbf{R}} & \mathbf{0}_{3 \times 3} \\ \dots & \dots & \dots \\ \mathbf{0}_{6 \times 9} & \vdots & \mathbf{0}_{6 \times 6} \end{bmatrix} \in \mathbb{R}^{15 \times 15}, \quad (\text{A.7})$$

where

$$\mathbf{2A} = \begin{bmatrix} \mathbf{0}_{3 \times 3} & \mathbf{0}_{3 \times 3} & \mathbf{0}_{3 \times 3} \\ \mathbf{g}^\wedge & \mathbf{0}_{3 \times 3} & \mathbf{0}_{3 \times 3} \\ \mathbf{0}_{3 \times 3} & \mathbf{I}_3 & \mathbf{0}_{3 \times 3} \end{bmatrix} \in \mathbb{R}^{9 \times 9} \quad (\text{A.8})$$

Position measurements formulated according to Equ. (30) are equivariant, yielding the following output matrix

$$\mathbf{C}^* = \left[\frac{1}{2} (y + \hat{\mathbf{p}})^\wedge \quad \mathbf{0}_{3 \times 3} \quad -\mathbf{I}_3 \quad \mathbf{0}_{3 \times 3} \quad \mathbf{0}_{3 \times 6} \right] \in \mathbb{R}^{3 \times 15}. \quad (\text{A.9})$$

It is trivial to verify that the state matrix in Equ. (A.7), derived according to equivariant filter design principles, directly corresponds to the state matrix in the Imperfect-IEKF [10, Sec. 7].

A.5 TG-EqF

A.5.1 Overview

The state space is defined as $\mathcal{M} := \mathcal{SE}_2(3) \times \mathbb{R}^9$ with $\xi := (\mathbf{T}, \mathbf{b}) \in \mathcal{M}$. One has $\mathbf{T} = (\mathbf{R}, \mathbf{v}, \mathbf{p}) \in \mathcal{SE}_2(3)$ and $\mathbf{b} = (\mathbf{b}_\omega, \mathbf{b}_a, \mathbf{b}_\nu) \in \mathbb{R}^9$. Choose the origin to be $\hat{\xi} = (\mathbf{I}_5, \mathbf{0}_{9 \times 1}) \in \mathcal{M}$. The velocity input is given by $u := (\boldsymbol{\omega}, \mathbf{a}, \boldsymbol{\nu}, \boldsymbol{\tau}_\omega, \boldsymbol{\tau}_a, \boldsymbol{\tau}_\nu)$.

The symmetry group of TG-EqF is given by $\mathbf{G}_{\text{TG}} : \mathbf{SE}_2(3) \times \mathfrak{se}_2(3)$. Define the filter state $\hat{X} = (\hat{C}, \hat{\gamma}) \in \mathbf{G}_{\text{TG}}$ with $\hat{C} = (\hat{A}, \hat{a}, \hat{b}) \in \mathbf{SE}_2(3)$ and $\hat{\gamma} = (\hat{\gamma}_\omega, \hat{\gamma}_a, \hat{\gamma}_\nu)^\wedge \in \mathfrak{se}_2(3)$. The state estimate is given by

$$\hat{\xi} := \phi(\hat{X}, \hat{\xi}) = (\hat{C}, \text{Ad}_{\hat{C}^{-1}}(-\hat{\gamma}^\vee)) = (\hat{\mathbf{T}}, \hat{\mathbf{b}}). \quad (\text{A.10})$$

The state error is defined as

$$e := \phi(\hat{X}^{-1}, \xi) = (\mathbf{T}\hat{C}^{-1}, \text{Ad}_{\hat{C}}^\vee(\mathbf{b} + \text{Ad}_{\hat{C}^{-1}}[\hat{\gamma}^\vee])) \quad (\text{A.11})$$

$$= (\mathbf{T}\hat{C}^{-1}, \text{Ad}_{\hat{C}}^\vee \mathbf{b} + \hat{\gamma}^\vee) \quad (\text{A.12})$$

$$= (\mathbf{T}\hat{\mathbf{T}}^{-1}, \text{Ad}_{\hat{\mathbf{T}}}^\vee(\mathbf{b} - \hat{\mathbf{b}})) \quad (\text{A.13})$$

A.5.2 Error dynamics

Navigation states The error dynamics related to Equ. (A.11) for the navigation states $e_T = \mathbf{T} \hat{\mathbf{T}}^{-1}$ is given by

$$\begin{aligned}\dot{e}_T &= \dot{\mathbf{T}} \hat{\mathbf{T}}^{-1} - \mathbf{T} \hat{\mathbf{T}}^{-1} \dot{\hat{\mathbf{T}}} \hat{\mathbf{T}}^{-1} \\ &= \mathbf{T}(\mathbf{W} - \mathbf{B} + \mathbf{D}) \hat{\mathbf{T}}^{-1} + (\mathbf{G} - \mathbf{D}) \mathbf{T} \hat{\mathbf{T}}^{-1} \\ &\quad - e_T \hat{\mathbf{T}}(\mathbf{W} - \hat{\mathbf{B}} + \mathbf{D}) \hat{\mathbf{T}}^{-1} - e_T(\mathbf{G} - \mathbf{D}) \hat{\mathbf{T}} \hat{\mathbf{T}}^{-1} \\ &= e_T \hat{\mathbf{T}}(\mathbf{W} - \mathbf{B} + \mathbf{D}) \hat{\mathbf{T}}^{-1} - e_T \hat{\mathbf{T}}(\mathbf{W} - \hat{\mathbf{B}} + \mathbf{D}) \hat{\mathbf{T}}^{-1} \\ &\quad + (\mathbf{G} - \mathbf{D})e_T - e_T(\mathbf{G} - \mathbf{D}) \\ &= e_T \text{Ad}_{\hat{\mathbf{T}}}[\hat{\mathbf{B}} - \mathbf{B}] + (\mathbf{G} - \mathbf{D})e_T - e_T(\mathbf{G} - \mathbf{D}).\end{aligned}$$

The above dynamics can be separate to two parts: $\dot{e}_T = \dot{e}_{T_W} + \dot{e}_{T_G}$, where $\dot{e}_{T_W} = e_T \text{Ad}_{\hat{\mathbf{T}}}[\hat{\mathbf{B}} - \mathbf{B}]$ and $\dot{e}_{T_G} = (\mathbf{G} - \mathbf{D})e_T - e_T(\mathbf{G} - \mathbf{D})$. The linearization can be derived separately for each part.

The local coordinate chart is given by $\varepsilon = \log \circ \phi_{\hat{\xi}}^{-1}(e)$. For each state, one has

$$\begin{aligned}e_T &= \exp_{\mathbf{SE}_2(3)}(\varepsilon_T^\wedge), \\ e_b &= \text{Ad}_{e_T^{-1}}[(-J_l(\varepsilon_T)\varepsilon_b)^\wedge],\end{aligned}$$

where the exponential map $\exp_{\mathbf{SE}_2(3) \times \mathfrak{se}_2(3)}$ is derived from the semi-direct product structure, and $J_l(\varepsilon_T)$ is the left Jacobian of $\mathbf{SE}_2(3)$, given by

$$J_l(\varepsilon_T) = \sum_{k=0}^{\infty} \frac{1}{(k+1)!} \text{ad}_{\varepsilon_T}^k.$$

Recall that by definition Equ. (A.11) one has $e_b^\wedge := \text{Ad}_{\hat{\mathbf{T}}}[(\mathbf{b} - \hat{\mathbf{b}})^\wedge]$ with $\mathbf{b}^\wedge = \mathbf{B}$, and $\hat{\mathbf{b}}^\wedge = \hat{\mathbf{B}}$. Hence, for \dot{e}_{T_W} one has

$$\dot{e}_{T_W} = e_T \text{Ad}_{\hat{\mathbf{T}}}[\hat{\mathbf{B}} - \mathbf{B}] = -e_T e_b^\wedge.$$

Substituting the local coordinate yields

$$\begin{aligned}\text{D exp}_{\mathbf{SE}_2(3)}(\varepsilon_T^\wedge)[\dot{e}_{T_W}^\wedge] &= -e_T \text{Ad}_{e_T^{-1}}[(-J_l(\varepsilon_T)\varepsilon_b)^\wedge] \\ e_T \frac{\mathbf{I} - \exp(-\text{ad}_{\varepsilon_T^\wedge})}{\text{ad}_{\varepsilon_T^\wedge}} \dot{e}_{T_W}^\wedge &= -e_T \text{Ad}_{e_T^{-1}}[(-J_l(\varepsilon_T)\varepsilon_b)^\wedge] \\ \text{Ad}_{e_T} \frac{\mathbf{I} - \exp(-\text{ad}_{\varepsilon_T^\wedge})}{\text{ad}_{\varepsilon_T^\wedge}} \dot{e}_{T_W}^\wedge &= (J_l(\varepsilon_T)\varepsilon_b)^\wedge.\end{aligned}\quad (\text{A.14})$$

Because $\text{Ad}_{e_T} = \text{Ad}_{\exp(\varepsilon_T^\wedge)} = \exp(\text{ad}_{\varepsilon_T^\wedge})$, the term on

the left side in Equ. (A.14) can be modified as

$$\begin{aligned}\text{Ad}_{e_T} \frac{\mathbf{I} - \exp(-\text{ad}_{\varepsilon_T^\wedge})}{\text{ad}_{\varepsilon_T^\wedge}} &= \exp(\text{ad}_{\varepsilon_T^\wedge}) \frac{\mathbf{I} - \exp(-\text{ad}_{\varepsilon_T^\wedge})}{\text{ad}_{\varepsilon_T^\wedge}} \\ &= \frac{\exp(\text{ad}_{\varepsilon_T^\wedge}) - \mathbf{I}}{\text{ad}_{\varepsilon_T^\wedge}} \quad (\text{Expanding exp,}) \\ &= \sum_{k=0}^{\infty} \frac{1}{(k+1)!} \text{ad}_{\varepsilon_T^\wedge}^k = J_l(\varepsilon_T).\end{aligned}\quad (\text{A.15})$$

Hence, for the linearization of \dot{e}_{T_W} , one has

$$\dot{e}_{T_W} = \varepsilon_b.$$

For the second part $\dot{e}_{T_G} = \text{D exp}_{\mathbf{SE}_2(3)}(\varepsilon_T^\wedge)[\dot{e}_{T_G}^\wedge]$, one has

$$e_T \frac{\mathbf{I} - \exp(-\text{ad}_{\varepsilon_T^\wedge})}{\text{ad}_{\varepsilon_T^\wedge}} \dot{e}_{T_G}^\wedge = \begin{bmatrix} \mathbf{0}_{3 \times 3} & \mathbf{g} - e_R \mathbf{g} & e_v \\ \mathbf{0}_{1 \times 3} & 0 & 0 \\ \mathbf{0}_{1 \times 3} & 0 & 0 \end{bmatrix}. \quad (\text{A.16})$$

Multiply both sides of Equ. (A.16) by e_T^{-1} and then apply Ad_{e_T} to both sides:

$$\begin{aligned}\text{Ad}_{e_T} \frac{\mathbf{I} - \exp(-\text{ad}_{\varepsilon_T^\wedge})}{\text{ad}_{\varepsilon_T^\wedge}} \dot{e}_{T_G} &= \text{Ad}_{e_T} e_T^{-1} \begin{bmatrix} \mathbf{0}_{3 \times 3} & \mathbf{g} - e_R \mathbf{g} & e_v \\ \mathbf{0}_{1 \times 3} & 0 & 0 \\ \mathbf{0}_{1 \times 3} & 0 & 0 \end{bmatrix} \\ &= \begin{bmatrix} \mathbf{0}_{3 \times 3} & \mathbf{g} - e_R \mathbf{g} & e_v \\ \mathbf{0}_{1 \times 3} & 0 & 0 \\ \mathbf{0}_{1 \times 3} & 0 & 0 \end{bmatrix}.\end{aligned}$$

Use the result from Equ. (A.15):

$$J_l(\varepsilon_T) \dot{e}_{T_G} = \begin{bmatrix} \mathbf{0}_{3 \times 3} & (\mathbf{I} - e_R) \mathbf{g} & J_l(\varepsilon_R) \varepsilon_v \\ \mathbf{0}_{1 \times 3} & 0 & 0 \\ \mathbf{0}_{1 \times 3} & 0 & 0 \end{bmatrix}. \quad (\text{A.17})$$

Note that:

$$\begin{aligned}\mathbf{I} - e_R &= \mathbf{I} - \exp(\varepsilon_R^\wedge) \\ &= \mathbf{I} - \sum_{k=0}^{\infty} \frac{1}{k!} \varepsilon_R^\wedge{}^k \\ &= -\left(\sum_{k=0}^{\infty} \frac{1}{(k+1)!} \varepsilon_R^\wedge{}^k \right) \varepsilon_R^\wedge \\ &= -J_l(\varepsilon_R) \varepsilon_R^\wedge.\end{aligned}$$

One can then simplify Equ. (A.17) to

$$\dot{\varepsilon}_{T_G} = \begin{bmatrix} \mathbf{0}_{3 \times 3} & \mathbf{g}^\wedge \varepsilon_R & \varepsilon_v \\ \mathbf{0}_{1 \times 3} & 0 & 0 \\ \mathbf{0}_{1 \times 3} & 0 & 0 \end{bmatrix}.$$

Combining the results for $\dot{\varepsilon}_{T_W}$ and $\dot{\varepsilon}_{T_G}$, one has

$$\dot{\varepsilon}_T = (\varepsilon_{b_\omega}, \varepsilon_{b_a} + \mathbf{g}^\wedge \varepsilon_R, \varepsilon_{b_\nu} + \varepsilon_v)^\wedge.$$

Bias states The linearization of the bias error are derived from the formula given by

$$\begin{aligned} \dot{\varepsilon} &= \mathbf{A}_t^0 \varepsilon + \mathcal{O}(\varepsilon^2), \\ \mathbf{A}_t^0 &= D_e|_\xi \vartheta(e) D_E|_I \phi_\xi(E) D_e|_\xi \Lambda(e, u^\circ) D_\varepsilon|_0 \vartheta^{-1}(\varepsilon). \end{aligned}$$

In this case, because we choose normal coordinates as the local coordinate chart, that is, $\vartheta := \log \circ \phi_\xi^{-1}$, we have

$$\dot{\varepsilon} = D_e|_\xi \Lambda(e, \hat{u}) D_E|_I \phi_\xi(E)[\varepsilon] + \mathcal{O}(\varepsilon^2).$$

Evaluating $D\phi_\xi$ at \mathbf{I} with direction $[\varepsilon_T, \varepsilon_b]$ yields

$$D\phi_\xi(\mathbf{I})[\varepsilon_T, \varepsilon_b] = (\varepsilon_T^\wedge, -\varepsilon_b^\wedge).$$

Evaluating $D\Lambda_{\hat{u}}$ at $\hat{\xi}$ with direction $[\varepsilon_T^\wedge, -\varepsilon_b^\wedge]$ yields

$$\begin{aligned} D\Lambda_{\hat{u}}(\hat{\xi})[\varepsilon_T^\wedge, -\varepsilon_b^\wedge] &= (\sim, \text{ad}_{-\varepsilon_b^\wedge} [\Lambda_1(\hat{\xi}, \hat{u})]) \\ &= (\sim, \mathbf{ad}_{(\hat{w}^\wedge + \mathbf{G})}^\vee \varepsilon_b). \end{aligned}$$

Hence the linearization of bias error is given by

$$\dot{\varepsilon}_b = \mathbf{ad}_{(\hat{w}^\wedge + \mathbf{G})}^\vee \varepsilon_b + \mathcal{O}(\varepsilon^2).$$

A.5.3 Filter design

The linearized error state matrix $\mathbf{A}_t^0 | \dot{\varepsilon} \simeq \mathbf{A}_t^0 \varepsilon$ is defined according to

$$\mathbf{A}_t^0 = \begin{bmatrix} \mathbf{2A} & \vdots & \mathbf{I}_9 \\ \cdots & \cdots & \cdots \\ \mathbf{0}_{9 \times 9} & \mathbf{ad}_{(\hat{w}^\wedge + \mathbf{G})}^\vee & \end{bmatrix} \in \mathbb{R}^{18 \times 18}, \quad (\text{A.18})$$

with $\mathbf{2A}$ in Equ. (A.8).

Position measurements formulated according to Equ. (30) are equivariant, yielding the following output matrix

$$\mathbf{C}^* = \left[\frac{1}{2} (y + \hat{p})^\wedge \mathbf{0}_{3 \times 3} \quad -\mathbf{I}_3 \quad \mathbf{0}_{3 \times 6} \quad \mathbf{0}_{3 \times 3} \right] \in \mathbb{R}^{3 \times 15}. \quad (\text{A.19})$$

Moreover, an additional constraint can be imposed on the virtual bias \mathbf{b}_ν ; that is, an additional measurement in the form of $h(\xi) = \mathbf{b}_\nu = \mathbf{0} \in \mathbb{R}^3$ can be considered, leading to the following output matrix

$$\mathbf{C}^0 = \left[\mathbf{0}_{3 \times 3} \quad \mathbf{0}_{3 \times 3} \quad \mathbf{0}_{3 \times 3} \quad -\hat{\mathbf{R}}^\top \quad \mathbf{0}_{3 \times 3} \quad \hat{\mathbf{R}}^\top \hat{\mathbf{p}}^\wedge \right] \in \mathbb{R}^{3 \times 15}. \quad (\text{A.20})$$

Note that for a practical implementation of the presented EqF the virtual inputs ν is set to zero.

It is worth noticing that the EqF built on the $\mathbf{G}_{\mathbf{TG}}$ symmetry group is the only filter with exact linearization of the navigation error dynamics.

A.6 DP-EqF

A.6.1 Overview

The state space is defined as $\mathcal{M} := \mathcal{HG}(3) \times \mathbb{R}^3 \times \mathbb{R}^6$ with $\xi := (\mathbf{T}, \mathbf{p}, \mathbf{b}) \in \mathcal{M}$. One has $\mathbf{T} = (\mathbf{R}, \mathbf{v}) \in \mathcal{HG}(3)$ and $\mathbf{b} = (\mathbf{b}_\omega, \mathbf{b}_a) \in \mathbb{R}^6$. Choose the origin to be $\hat{\xi} = (\mathbf{I}_4, \mathbf{0}_{6 \times 1}, \mathbf{0}_{3 \times 1}) \in \mathcal{M}$. The velocity input is given by $u := (\boldsymbol{\omega}, \mathbf{a}, \boldsymbol{\tau}_\omega, \boldsymbol{\tau}_a, \boldsymbol{\nu})$.

The symmetry group of DP-EqF is given by $\mathbf{G}_{\mathbf{DP}} : \mathbf{HG}(3) \times \mathfrak{hg}(3) \times \mathbb{R}^3$. Define the filter state $\hat{X} = (\hat{B}, \hat{\beta}, \hat{c}) \in \mathbf{G}_{\mathbf{DP}}$ with $\hat{B} = (\hat{A}, \hat{a}) \in \mathbf{HG}(3)$ and $\hat{\beta} = (\hat{\beta}_\omega, \hat{\beta}_a)^\wedge \in \mathfrak{hg}(3)$. The state estimate is given by

$$\hat{\xi} := \phi(\hat{X}, \hat{\xi}) = (\hat{B}, \text{Ad}_{\hat{B}^{-1}}(-\hat{\beta}), \hat{c}) = (\hat{\mathbf{T}}, \hat{\mathbf{b}}, \hat{\mathbf{p}}). \quad (\text{A.21})$$

The state error is defined as

$$e := \phi(\hat{X}^{-1}, \xi) = (\mathbf{T} \hat{B}^{-1}, \mathbf{Ad}_{\hat{B}}^\vee \mathbf{b} + \hat{\beta}^\vee, \mathbf{p} - \hat{c}) \quad (\text{A.22})$$

$$= (\mathbf{T} \hat{\mathbf{T}}^{-1}, \mathbf{Ad}_{\hat{\mathbf{T}}}^\vee (\mathbf{b} - \hat{\mathbf{b}}), \mathbf{p} - \hat{\mathbf{p}}) \quad (\text{A.23})$$

A.6.2 Error dynamics

Navigation states Because of the semi-direct product structure related to the rotation and velocity states and the corresponding bias states, the derivation of the error dynamics of the $\mathcal{HG}(3)$ part is similar to the one in TG-EqF. In this case, one has

$$\begin{aligned} \dot{\varepsilon}_R &= \varepsilon_{b_\omega}, \\ \dot{\varepsilon}_v &= \varepsilon_{b_a} + \mathbf{g}^\wedge \varepsilon_R. \end{aligned}$$

For the position error, one has

$$\begin{aligned}
\dot{\hat{e}}_p &= \dot{e}_p = \dot{\hat{\mathbf{p}}} - \dot{\mathbf{p}} = \mathbf{R} \boldsymbol{\nu} + \mathbf{v} - \hat{\mathbf{R}} \boldsymbol{\nu} - \hat{\mathbf{v}} \\
&= e_v + e_R \hat{\mathbf{v}} - \hat{\mathbf{v}} + e_R \hat{\mathbf{R}} \boldsymbol{\nu} - \hat{\mathbf{R}} \boldsymbol{\nu} \\
&= J_l(\varepsilon_R) \varepsilon_v + (\mathbf{I} + \varepsilon_R^\wedge + O(\varepsilon_R^2)) (\hat{\mathbf{R}} \boldsymbol{\nu} + \hat{\mathbf{v}}) - (\hat{\mathbf{R}} \boldsymbol{\nu} + \hat{\mathbf{v}}) \\
&= J_l(\varepsilon_R) \varepsilon_v + (\mathbf{I} + \varepsilon_R^\wedge + O(\varepsilon_R^2)) \hat{\mathbf{v}} - \hat{\mathbf{v}} \\
&= \varepsilon_v - \hat{\mathbf{v}}^\wedge \varepsilon_R + O(\varepsilon^2).
\end{aligned}$$

Bias states The derivation of bias error dynamics is the same as TG-EqF:

$$\dot{\hat{e}}_b = \mathbf{ad}_{(\hat{\mathbf{w}}^\wedge + \mathbf{G})}^\vee \varepsilon_b + O(\varepsilon^2).$$

A.6.3 Filter design

The linearized error state matrix $\mathbf{A}_t^0 \mid \dot{\hat{e}} \simeq \mathbf{A}_t^0 \varepsilon$ is defined according to

$$\mathbf{A}_t^0 = \begin{bmatrix} {}_3\mathbf{A} & \mathbf{I}_6 & \mathbf{0}_{6 \times 3} \\ \mathbf{0}_{6 \times 6} & \mathbf{ad}_{(\hat{\mathbf{w}}^\wedge + \mathbf{G})}^\vee & \mathbf{0}_{6 \times 3} \\ {}_4\mathbf{A} & \mathbf{0}_{3 \times 6} & \mathbf{0}_{3 \times 3} \end{bmatrix} \in \mathbb{R}^{15 \times 15}, \quad (\text{A.24})$$

where

$$\begin{aligned}
{}_3\mathbf{A} &= \begin{bmatrix} \mathbf{0}_{3 \times 3} & \mathbf{0}_{3 \times 3} \\ \mathbf{g}^\wedge & \mathbf{0}_{3 \times 3} \end{bmatrix} \in \mathbb{R}^{6 \times 6} \\
{}_4\mathbf{A} &= \begin{bmatrix} -\hat{\mathbf{v}}^\wedge & \mathbf{I}_3 \end{bmatrix} \in \mathbb{R}^{3 \times 6}.
\end{aligned}$$

Position measurements are linear; therefore, the output matrix is written

$$\mathbf{C}^0 = \begin{bmatrix} \mathbf{0}_{3 \times 3} & \mathbf{0}_{3 \times 3} & \mathbf{0}_{3 \times 6} & \mathbf{I}_3 & \mathbf{0}_{3 \times 3} \end{bmatrix} \in \mathbb{R}^{3 \times 15}. \quad (\text{A.25})$$

Similar to the previous filter, for a practical implementation of the presented EqF, the virtual input $\boldsymbol{\nu}$ is set to zero.

A.7 SD-EqF

A.7.1 Overview

The state space is defined as $\mathcal{M} := \mathcal{SE}_2(3) \times \mathbb{R}^6$ with $\xi := (\mathbf{T}, \mathbf{b}) \in \mathcal{M}$. One has $\mathbf{T} = (\mathbf{R}, \mathbf{v}, \mathbf{p}) \in \mathcal{SE}_2(3)$ and $\mathbf{b} = (\mathbf{b}_\omega, \mathbf{b}_a) \in \mathbb{R}^6$. Choose the origin to be $\hat{\xi} = (\mathbf{I}_5, \mathbf{0}_{6 \times 1}) \in \mathcal{M}$. The velocity input is given by $u := (\boldsymbol{\omega}, \mathbf{a}, \boldsymbol{\tau}_\omega, \boldsymbol{\tau}_a)$.

The symmetry group of TG-EqF is given by $\mathbf{G}_{\text{SD}} : \mathbf{SE}_2(3) \times \mathfrak{se}(3)$. Define the filter state $\hat{X} = (\hat{C}, \hat{\gamma}) \in \mathbf{G}_{\text{SD}}$ with $\hat{C} = (\hat{A}, \hat{a}, \hat{b}) \in \mathbf{SE}_2(3)$ and $\hat{\gamma} = (\hat{\gamma}_\omega, \hat{\gamma}_a)^\wedge \in \mathfrak{se}(3)$. The $\mathbf{SE}_2(3)$ component in \hat{X} can also be expressed in $\hat{C} = (\hat{B}, \hat{b})$ where $\hat{B} = (\hat{A}, \hat{a}) \in \mathbf{HG}(3)$. The state estimate is given by

$$\hat{\xi} := \phi(\hat{X}, \hat{\xi}) = (\hat{C}, \text{Ad}_{\hat{B}^{-1}}(-\hat{\gamma}^\vee)) = (\hat{\mathbf{T}}, \hat{\mathbf{b}}). \quad (\text{A.26})$$

The state error is defined as

$$e := \phi(\hat{X}^{-1}, \xi) = (\mathbf{T} \hat{C}^{-1}, \mathbf{Ad}_{\hat{B}}^\vee(\mathbf{b} + \text{Ad}_{\hat{B}^{-1}}[\hat{\gamma}^\vee])) \quad (\text{A.27})$$

$$= (\mathbf{T} \hat{C}^{-1}, \mathbf{Ad}_{\hat{B}}^\vee \mathbf{b} + \hat{\gamma}^\vee). \quad (\text{A.28})$$

A.7.2 Error dynamics

Navigation states Because of the semi-direct product structure related to the rotation and velocity states and the corresponding bias states, the derivation of the error dynamics of the $\mathbf{HG}(3)$ part is similar to the one in TG-EqF. In this case, one has

$$\begin{aligned}
\dot{e}_R &= \varepsilon_{b_\omega}, \\
\dot{e}_v &= \varepsilon_{b_a} + \mathbf{g}^\wedge \varepsilon_R.
\end{aligned}$$

For the position error $\dot{e}_p = \dot{\hat{e}}_p + O(\varepsilon^2)$, one has

$$\begin{aligned}
\dot{e}_p &= \frac{d}{dt}(-\mathbf{R} \hat{\mathbf{R}}^\top \hat{\mathbf{p}} + \mathbf{p}) \\
&= -\dot{e}_R \hat{\mathbf{p}} - e_R \dot{\hat{\mathbf{p}}} + \dot{\mathbf{p}} \\
&= e_R e_{b_\omega}^\wedge \hat{\mathbf{p}} - e_R \hat{\mathbf{v}} + \mathbf{v} \\
\dot{e}_p &= ((\mathbf{I} + \varepsilon_R^\wedge + O(\varepsilon^2))) (\mathbf{I} + \varepsilon_{b_\omega}^\wedge + O(\varepsilon^2)) \hat{\mathbf{p}} + (\varepsilon_v + O(\varepsilon^2)) \\
&= \varepsilon_v + \hat{\mathbf{p}}^\wedge \varepsilon_{b_\omega} + O(\varepsilon^2).
\end{aligned}$$

Bias states The derivation of bias error dynamics is the same as TG-EqF, and yields:

$$\dot{\hat{e}}_b = \mathbf{ad}_{(\mathbf{Ad}_{\hat{B}}^\vee \mathbf{w} + \hat{\gamma}^\vee + \mathbf{G}^\vee)}^\vee \varepsilon_b + O(\varepsilon^2).$$

Note that the following relation holds

$$\mathbf{Ad}_{\hat{B}}^\vee \mathbf{w} + \hat{\gamma}^\vee = \Pi(\hat{\mathbf{w}}^\wedge)^\vee,$$

References

- [1] A Barrau and S Bonnabel. The Invariant Extended Kalman Filter as a Stable Observer. *IEEE Transactions on Automatic Control*, 62(4):1797–1812, 2017.
- [2] Axel Barrau and Axel Barrau. *Non-linear state error based extended Kalman filters with applications to navigation*. PhD thesis, Mines Paristech, 9 2015.
- [3] Axel Barrau and Silvere Bonnabel. The Geometry of Navigation Problems. *IEEE Transactions on Automatic Control*, 2022.
- [4] Christian Brommer, Alessandro Fornasier, Martin Scheiber, Jeff Delaune, Roland Brockers, Jan Steinbrener, and Stephan Weiss. INSANE: Cross-Domain UAV Data Sets with Increased Number of Sensors for developing Advanced and Novel Estimators. 10 2022.
- [5] Martin Brossard, Axel Barrau, Paul Chauchat, and Silvere Bonnabel. Associating Uncertainty to Extended Poses for on Lie Group IMU Preintegration With Rotating Earth. *IEEE Transactions on Robotics*, 2021.
- [6] Michael Burri, Janosch Nikolic, Pascal Gohl, Thomas Schneider, Joern Rehder, Sammy Omari, Markus W. Achtelik, and Roland Siegwart. The EuRoC micro aerial vehicle datasets. <https://doi.org/10.1177/0278364915620033>, 35(10):1157–1163, 1 2016.
- [7] Gregory S Chirikjian. *Stochastic models, information theory, and Lie groups, volume 2: Analytic methods and modern applications*, volume 2. Springer Science & Business Media, 2011.
- [8] Alessandro Fornasier, Yonhon Ng, Christian Brommer, Christoph Bohm, Robert Mahony, and Stephan Weiss. Overcoming Bias: Equivariant Filter Design for Biased Attitude Estimation With Online Calibration. *IEEE Robotics and Automation Letters*, 7(4):12118–12125, 10 2022.
- [9] Alessandro Fornasier, Yonhon Ng, Robert Mahony, and Stephan Weiss. Equivariant Filter Design for Inertial Navigation Systems with Input Measurement Biases. *2022 International Conference on Robotics and Automation (ICRA)*, pages 4333–4339, 5 2022.
- [10] Ross Hartley, Maani Ghaffari, Ryan M Eustice, and Jessy W Grizzle. Contact-aided invariant extended Kalman filtering for robot state estimation. *The International Journal of Robotics Research*, 39(4):402–430, 2020.
- [11] Simon J. Julier and Joseph J. LaViola. On Kalman filtering with nonlinear equality constraints. *IEEE Transactions on Signal Processing*, 55(6 II):2774–2784, 6 2007.
- [12] E. J. Lefferts, F. L. Markley, and M. D. Shuster. Kalman Filtering for Spacecraft Attitude Estimation. <https://doi.org/10.2514/3.56190>, 5(5):417–429, 5 1982.
- [13] X. Rong Li, Zhanlue Zhao, and Xiao Bai Li. Evaluation of Estimation Algorithms: Credibility Tests. *IEEE Transactions on Systems, Man, and Cybernetics Part A: Systems and Humans*, 42(1):147–163, 2012.
- [14] Xinghan Li, Haodong Jiang, Xingyu Chen, He Kong, and Junfeng Wu. Closed-Form Error Propagation on SE-n (3) Group for Invariant EKF With Applications to VINS. *IEEE Robotics and Automation Letters*, 7(4):10705–10712, 10 2022.
- [15] Robert Mahony, Tarek Hamel, and Jochen Trumpf. Equivariant systems theory and observer design. *arXiv*, 2020.
- [16] Robert Mahony, Jochen Trumpf, and Tarek Hamel. Observers for kinematic systems with symmetry? *IFAC Proceedings Volumes (IFAC-PapersOnline)*, 9(PART 1):617–633, 2013.
- [17] Robert Mahony, Pieter van Goor, and Tarek Hamel. Observer design for nonlinear systems with equivariance. *Annual Review of Control, Robotics, and Autonomous Systems*, 5:221–252, 2022.
- [18] Robert Mahony, Pieter Van Goor, and Tarek Hamel. Observer Design for Nonlinear Systems with Equivariance. <https://doi.org/10.1146/annurev-control-061520-010324>, 5:221–252, 5 2022.
- [19] Yonhon Ng, Pieter Van Goor, Tarek Hamel, and Robert Mahony. Equivariant Systems Theory and Observer Design for Second Order Kinematic Systems on Matrix Lie Groups. *Proceedings of the IEEE Conference on Decision and Control*, 2020-Decem(Xx):4194–4199, 2020.
- [20] Yonhon Ng, Pieter van Goor, and Robert Mahony. Pose Observation for Second Order Pose Kinematics. *IFAC-PapersOnLine*, 53(2):2317–2323, 1 2020.
- [21] Yonhon Ng, Pieter Van Goor, Robert Mahony, and Tarek Hamel. Attitude Observation for Second Order Attitude Kinematics. In *Proceedings of the IEEE Conference on Decision and Control*, volume 2019-Decem, pages 2536–2542. IEEE, 2019.
- [22] Natalia Pavlasek, Alex Walsh, and James Richard Forbes. Invariant Extended Kalman Filtering Using Two Position Receivers for Extended Pose Estimation. In *2021 IEEE International Conference on Robotics and Automation (ICRA)*, pages 5582–5588. Institute of Electrical and Electronics Engineers (IEEE), 10 2021.
- [23] Joan Solà. Quaternion kinematics for the error-state Kalman filter. 11 2017.
- [24] Pieter Van Goor, Tarek Hamel, and Robert Mahony. Equivariant Filter (EqF): A General Filter Design for Systems on Homogeneous Spaces. *Proceedings of the IEEE Conference on Decision and Control*, 2020-Decem(Cdc):5401–5408, 2020.
- [25] Pieter van Goor, Tarek Hamel, and Robert Mahony. Equivariant Filter (EqF). *IEEE Transactions on Automatic Control*, 6 2022.